ABSTRACT

VOLUME OPTIMIZATION OF A SIMPLE PLANETARY GEAR SET

By

Jeremy J. Deake

August 2014

This thesis describes a custom algorithm developed to optimize a simple planetary gear set. The optimization minimizes volume for one simple planetary gear set using American Gear Manufacturers Association stress equations, custom design constraints, and material constraints. Through predetermined reactions to adjustments, component features and planetary variables are modified systematically to obtain the target solution. This thesis demonstrates that the defined approach is an effective means of balancing all three components of a simple planetary gear set, thus resulting in a solution that has been optimized for volume.

VOLUME OPTIMIZATION OF A SIMPLE PLANETARY GEAR SET

A THESIS

Presented to the Department of Mechanical and Aerospace Engineering

California State University, Long Beach

In Partial Fulfillment

of the Requirements for the Degree

Master of Science in Mechanical Engineering

Committee Members:

Joshua Hamel, Ph.D. (Chair)
Panadda Marayon, Ph.D.
Praveen Shankar, Ph.D.

College Designee:

Antonella Sciortino, Ph.D.

By Jeremy J. Deake

B.S., 2005, Polytechnic University of California, Pomona

August 2014

ProQuest LLC.
789 East Eisenhower Parkway
P.O. Box 1346
Ann Arbor, MI 48106 - 1346

ACKNOWLEDGEMENTS

I would like to thank Anngwo Wang for his willingness to provide support, lend an ear for conceptual ideas, and provide information on gear standards and specifications. His assistance was instrumental in learning the gear fundamentals necessary for developing this thesis.

I would also like to thank MOOG for providing me the opportunity to work on a topic that may contribute to the industry and giving me the time necessary to complete this first step in a potentially very productive direction.

Finally I would like to thank my parents, Mary Ann and Doug Walker, for their unwavering support during this undertaking.

TABLE OF CONTENTS

LIST OF TABLES

LIST OF FIGURES

FIGURE Page

LIST OF ABBREVIATIONS

SPGS	Simple Planetary Gear Set
J1	Bending Geometry Factor Sun
J2	Bending Geometry Factor Planet
J3	Bending Geometry Factor Ring
I12	Contact Geometry Factor Sun to Planet
I23	Contact Geometry Factor Planet to Ring
AGMA	American Gear Manufacturers Association

CHAPTER 1

INTRODUCTION

In aerospace and mechanical engineering envelope, weight, and performance are among the key factors that drive design decisions. Along with cost and schedule, these factors are vital in completing a competitive design capable of winning a contract. In the aerospace actuation business, geared mechanisms make up a significant portion of aircraft components. Among these components, a simple planetary gear set (SPGS) is a compact and effective method of delivering actuation requirements.

To achieve compact and lightweight designs, component weight and envelope are minimized to meet the specific life and margin requirements. This is especially true for SPGSs as they are significant drivers of envelope and weight. The process of effectively sizing SPGSs can be cumbersome. There are many variables that when altered affect the stress of the individual gear components. Manual optimization is simply too cumbersome to be an effective design tool in industry applications.

Significant work has been completed to date on gear optimization and design. Both existing and unique algorithms have been applied to spur and helical offset gears, and multi stage offset gearboxes. Theses optimization techniques range from minimizing weight of a gear mesh, to minimizing weight and volume of a gearbox and its components.

This thesis builds on current work by expanding optimization to a SPGS and each of its geared components. The focus is on streamlining the design process of a SPGS by developing an optimization algorithm. The scope of the algorithm designed in this thesis is such that basic gear geometry information and material selection has already been completed. The algorithm optimizes the SPGS to minimize size and weight within the constraints provided by the designer. The fundamental approach and results of the algorithm are discussed and reviewed. Although the examples presented herein are for spur gears, the theory and technique can be used for helical, bevel, face, or other gear types as well. Expansion of scope and future works will be elaborated following the results discussion.

CHAPTER 2

BACKGROUND

Previous Works

Numerous works have been completed in the area of spur gear optimization. These works range from gearbox assemblies which optimize shafts, bearings, and offset gears, to single and multi stage offset gears, and a range of optimization techniques.

Marjonovic and others in their 2012 study [1] formulated a procedure to optimize multi stage offset spur gears. They presented a custom procedure to optimize the gear ratios of the gear train as well as the offset gearing shaft positions to minimize weight and envelope. Zhong and Shaojun in their 2013 study [2] presented an optimization technique for offset spur gears. Mendi and others in their 2010 study [3] presented a genetic algorithm to optimize a shaft, bearing, and offset spur gear to minimize the volume of the system. Savsani and others in their 2010 study [4] analyzed particle swarm and simulated annealing algorithms to minimize weight of an offset spur gear train. Similarly, Gologlu and Zeyveli in their 2009 study [5] presented a preliminary design technique to optimize the weight of an offset spur gear train using a genetic algorithm. In 1994 Savage and others [6] presented an optimization using a modified feasible directions search algorithm to minimize weight of an offset spur gear, bearings, and shafts.

As a result of their compact design and in-line assembly, SPGSs are a common approach to gear reduction in the automotive and aircraft industries. This thesis focuses on the optimization of one SPGS, simultaneously analyzing each gear in the planetary system. This thesis does not use an established algorithm to perform optimization. The genetic and particle swarm algorithms incorporate random generation of variables to explore alternate solutions. Simulated annealing searches for solutions in multiple directions from initial conditions, regardless of local results to ensure a global optimization is reached. This thesis describes the changes that occur in a SPGS as a result of specific predetermined variable adjustments. Because reactions of these changes are quantified by magnitude and direction, established algorithms that employ random generation or multi-directional changes are not necessary and inefficient. Optimization is instead performed using a custom algorithm tailored to the predetermined variable adjustments of the SPGS.

Basics of Spur Gears and Planetary Gearing

The basic principle of gearing is to provide a constant torque and speed ratio between two rotating components. This relationship is defined as conjugate gearing and is accomplished with the involute profile. Figure 1 below illustrates the generation of an involute profile. As seen in the figure, the involute is generated off of the gear base circle diameter by "un-wrapping" the base circle circumference and maintaining tangency to the base circle. This profile provides a constant line of action (see Figure 3 below) between mating gears at any location.

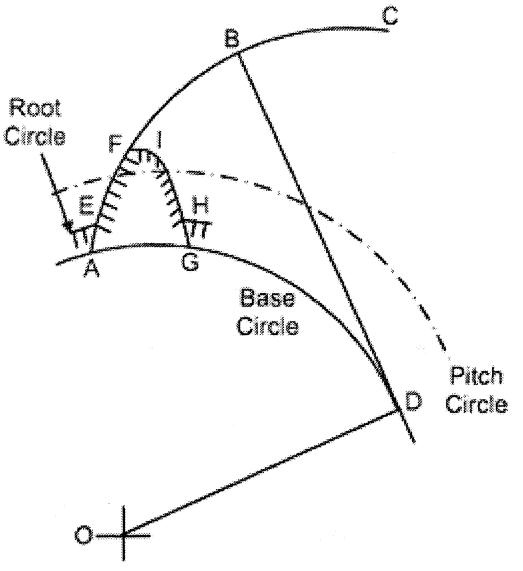

FIGURE 1. Geometric generation of an involute profile [14].

The spur gear is the simplest application of gearing. In incorporates straight teeth with a face generated by an involute profile that can be mounted externally or internally. Spur gear geometry and fundamental features are shown below in Figures 2, 3, and 4.

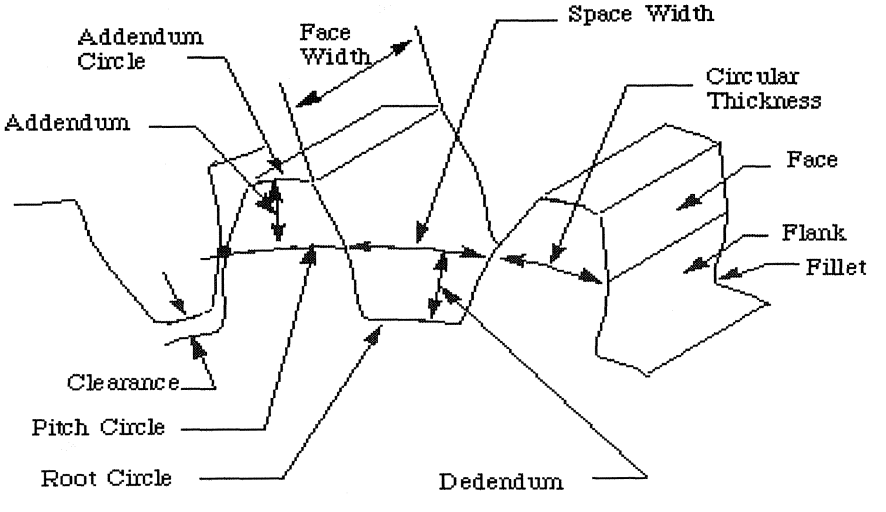

FIGURE 2. Fundamental spur gear geometry and features [13].

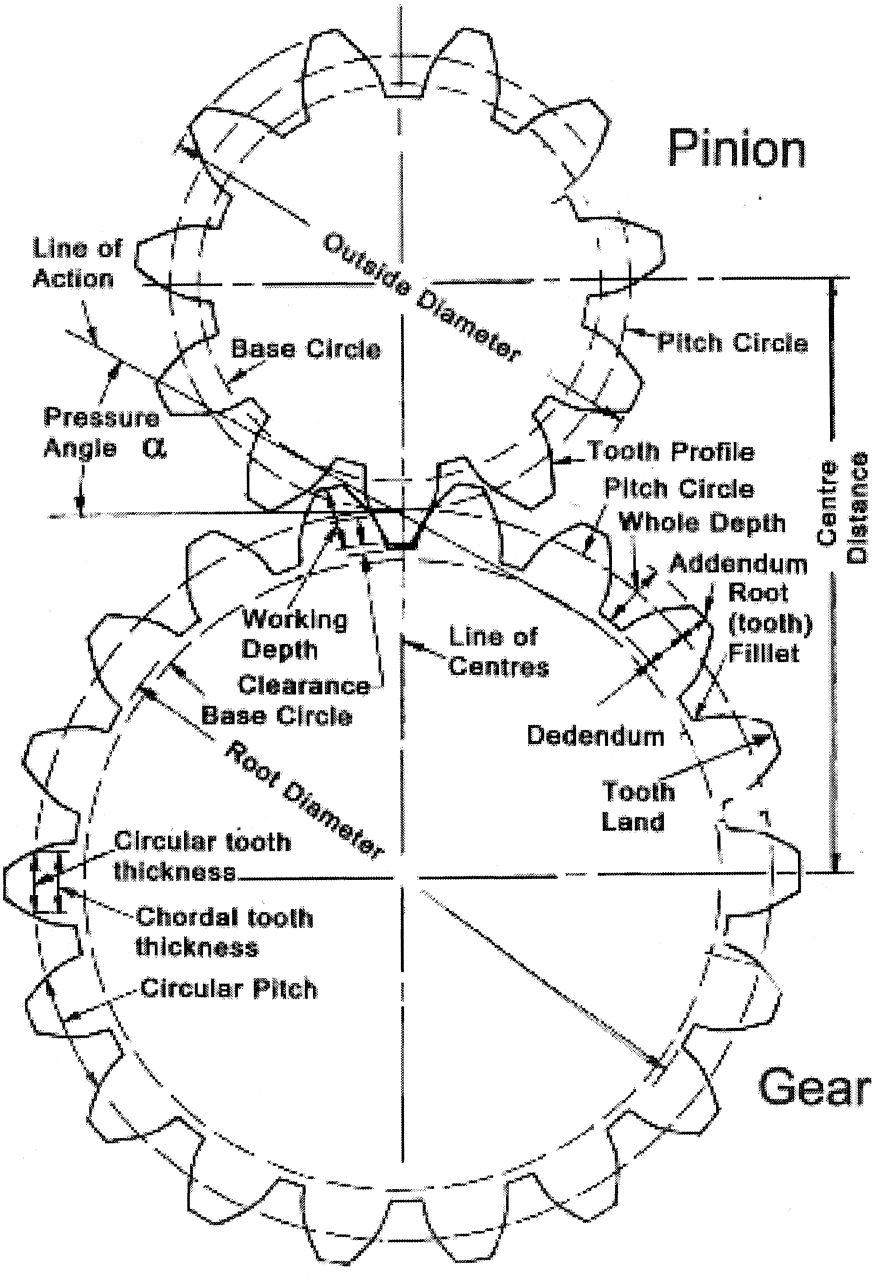

FIGURE 3. Fundamental spur gear geometry and features for an external gear mesh [12].

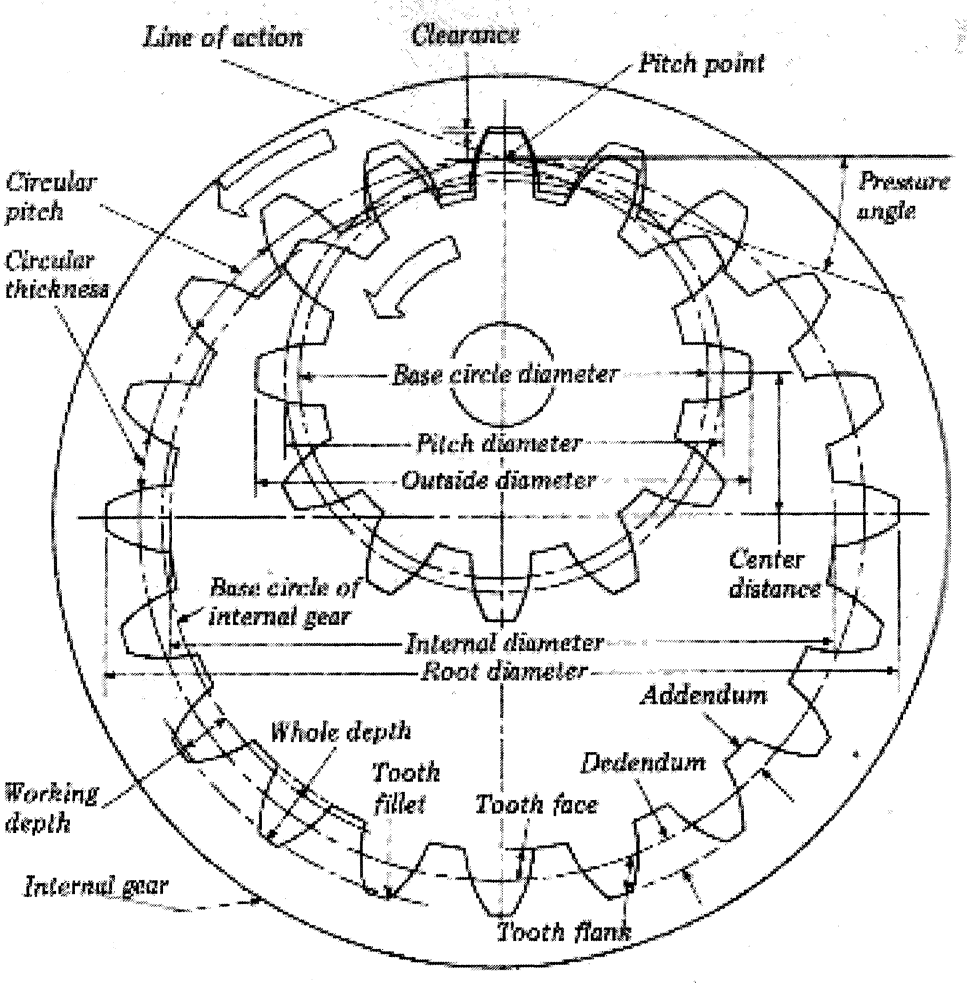

FIGURE 4. Fundamental spur gear geometry and features for an internal gear mesh [12].

Helical gears are similar to spur gears in that they transmit motion and torque in the same way, using gear teeth with involute profiles. However the length of the tooth for helical gears are angled with respect to the axis of the gear. This angled gear tooth is "wrapped" around the gear axis to form the helical gear tooth (see Figure 5). When compared to spur gears helical gears have more teeth in contact at any given moment and thus are quieter, and have lower contact and bending stress. However, helical gears have increased sliding which makes them less efficient than spur gears.

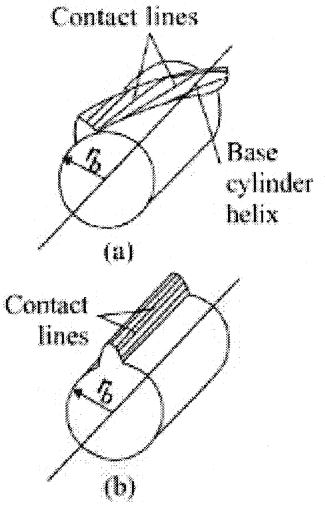

FIGURE 5. Helical gear tooth illustration [15].

SPGSs consist of a sun gear (sun), planet gear (planet), and ring gear (ring). The planet gears are typically constrained with a structural member called a carrier. There does exist variations of SPGSs that do not employ carriers, however those variations will not be discussed herein. An example of a SPGS is seen below in Figure 6.

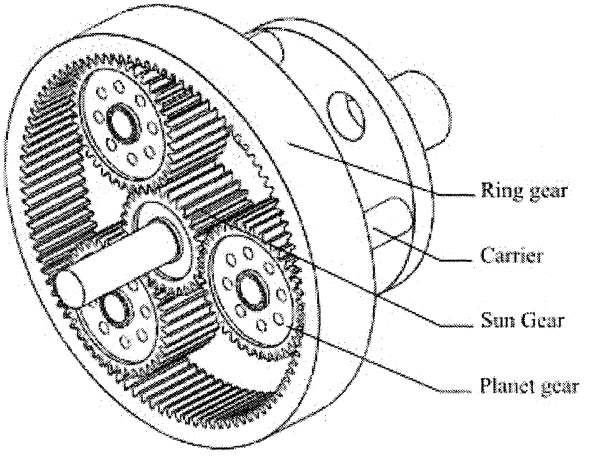

FIGURE 6. Simple planetary gear set [11].

The sun, carrier, and ring are the 3 components of a SPGS. For each of these components, when one of them is an input there are two possible outputs. This results in 6 possible configurations. These configurations and gear ratios are shown below in Figure 7 and Table 1.

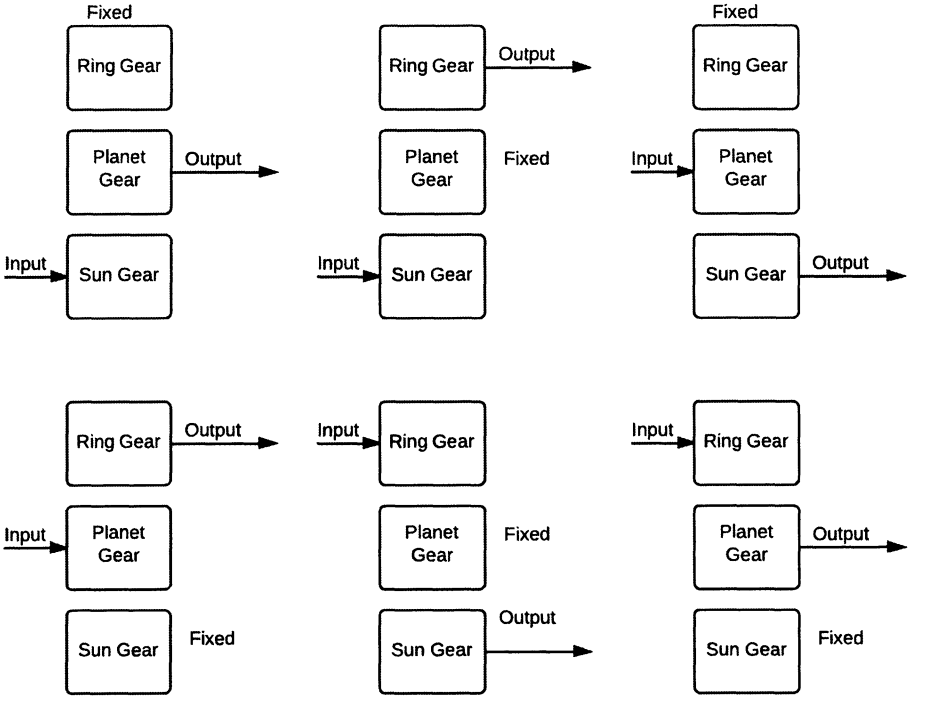

FIGURE 7. Input and output configurations for a SPGS.

TABLE 1. Gear Ratios for SPGS Configurations

Input	Output	Fixed	Ratio
S	C	R	1+R/S
S	R	C	(-)R/S
C	S	R	1/(1+R/S)
C	R	S	1/(1+S/R)
R	S	C	(-)S/R
R	C	S	1+S/R

Note that one member is always fixed. This is required to prevent the gear train from acting as a speed summing or differential gear train (two inputs and one output or one input and two outputs respectively). The gear ratios discussed in this thesis are applicable to a fixed ring, input at the sun, and output at the carrier. The optimization techniques discussed may be used on any input/output combination with minor adjustments for gear ratio equations. In addition, this thesis focuses on spur gears. The optimization techniques developed can be applied to helical gears as well by using the appropriate bending and contact geometry factor equations. The bending and contact geometry factors are discussed below.

To determine gear stress AGMA equations for bending and contact stress are used. The variables for the stress equations are defined in Table 2 below. These equations are:

$$\sigma = W^t K_o K_v K_s \frac{P_d}{F} \frac{K_M K_B}{J} \quad \text{.....Tooth Bending Stress [10]}$$

$$\sigma_c = C_p \sqrt{W^t K_o K_v K_s \frac{K_M}{d_p F} \frac{C_f}{I}} \quad \text{.....Tooth Contact Stress [10]}$$

TABLE 2. Bending and Contact Stress Equation Variables

W^t	Tangential Transmitted Load
K_o	Overload Factor
K_v	Dynamic Factor
K_s	Size Factor
K_m	Load Distribution Factor
K_B	Rim Thickness Factor
P_d	Transverse Diametral Pitch
F	Face Width
C_p	Elastic Coefficient
C_f	Surface Condition Factor
d_p	Operating Pitch Diameter Pinion

TABLE 2. Continued

J	Bending Geometry Factor
I	Contact Geometry Factor

The American Gear Manufacturers Association (AGMA) 908-B89 information sheet defines the bending and contact geometry factors. The bending geometry factor is defined for the sun (J1) planet (J2) and ring (J3). The contact geometry factor is defined from the sun to the planet (I12) and the planet to the ring (I23). Because of the large scope and complexity that goes into calculating the bending and contact geometry factors, the equations will not be discussed in this thesis.

The tooth bending and contact stress is most significantly affected by the bending and contact geometry factors, transverse diametral pitch, and face width. Therefore these variables are the focus of optimization in this work.

CHAPTER 3

SIMPLE PLANETARY OPTIMIZATION

Overview of Optimization Technique

The SPGS optimization is separated into modularized functions that are represented by block diagrams. The top-level optimization block diagram encompasses all of the sub level block diagrams and is shown below in Figure 8. This block runs all gear tooth combinations such that the sun gear is varied from 5 to 30 teeth. Subsequently the target gear ratio is calculated, the SPGS is checked for symmetric assembly, the SPGS component gear ratios are verified, and the geometry factor, diametral pitch, and face width blocks are executed. For each gear tooth combination all results are stored.

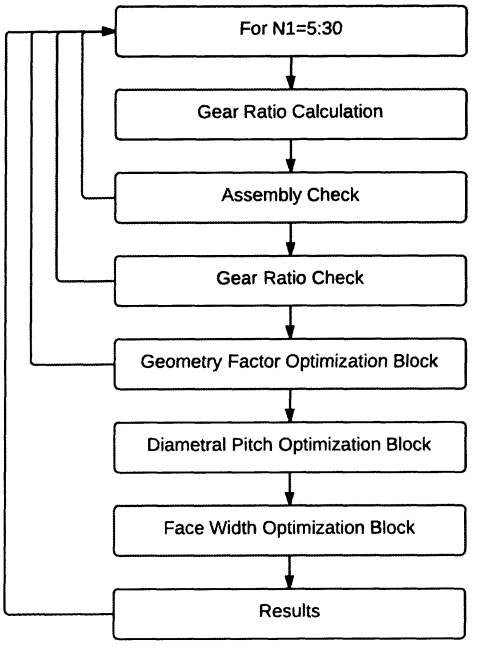

FIGURE 8. Top-level optimization block diagram.

The geometry optimization block diagram is shown below in Figure 9. This block maximizes J1, J2, and I12, while maintaining a target ratio between J1 and J2. The block also adjusts component addendums and dedendums to further increase J1, J2, and J3.

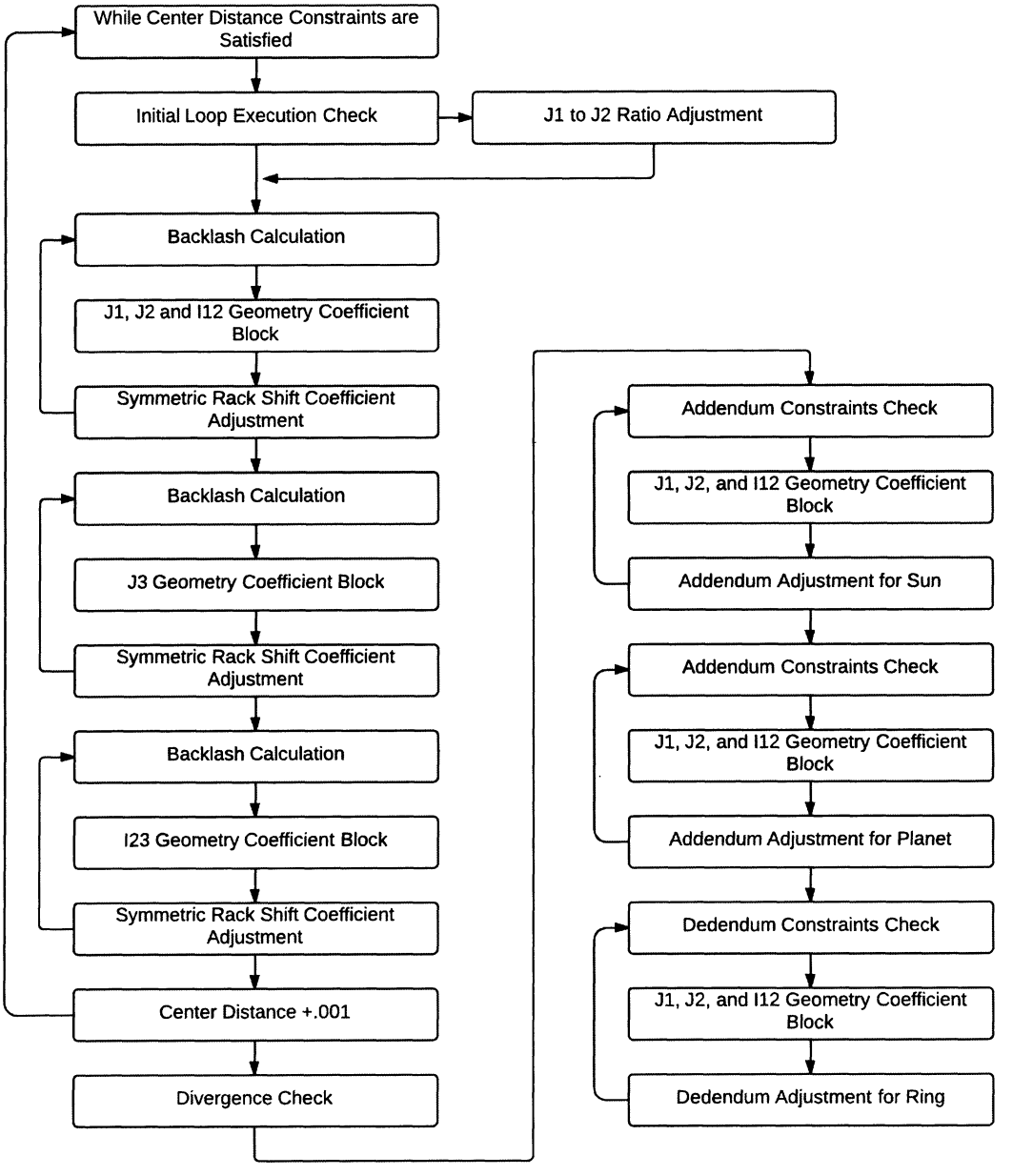

FIGURE 9. Geometry factor optimization block diagram.

Finally, the diametral pitch and face width optimization block diagrams are shown below in Figure 10. The diametral pitch block varies the diametral pitch such that the gear teeth are made increasingly small until allowable stresses are approached. Similarly, the face width optimization block decreases the face to bring the stresses even closer to the allowable values.

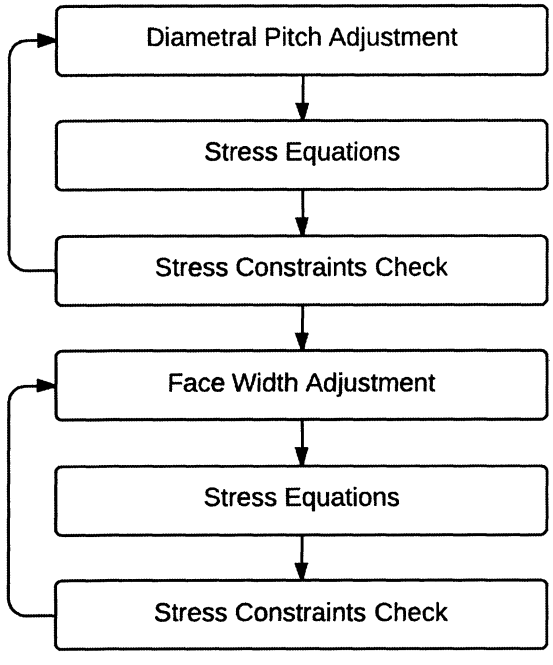

FIGURE 10. Diametral pitch and face width optimization block.

The result of this algorithm execution is a range of different sized SPGSs that all meet assembly, clearance, gear ratio, and stress requirements. The smallest SPGS can then be selected.

Detailed Optimization Approach

Prior to running the optimization algorithm all required inputs must be defined. These inputs are listed below in Table 3. Note: normalized values are made dimensionless by multiplying the value by the normal diametral pitch.

TABLE 3. Required Algorithm Inputs

$\sigma_{b1,all}$	Allowable Bending Stress Sun Gear (psi)
$\sigma_{b2,all}$	Allowable Bending Stress Planet Gear (psi)
$\sigma_{b3,all}$	Allowable Bending Stress Ring Gear (psi)
$\sigma_{c1,all}$	Allowable Contact Stress Sun Gear (psi)
$\sigma_{c2,all}$	Allowable Contact Stress Planet Gear (psi)
$\sigma_{c3,all}$	Allowable Contact Stress Ring Gear (psi)
ν_1	Poisson's Ration Sun Gear
ν_2	Poisson's Ration Planet Gear
ν_3	Poisson's Ration Ring Gear
E_1	Modulus of Elasticity Sun Gear (psi)
E_2	Modulus of Elasticity Planet Gear (psi)
E_3	Modulus of Elasticity Ring Gear (psi)
TL_1	Minimum Top Land or Sun (normalized)
TL_2	Minimum Top Land or Planet (normalized)
TL_3	Minimum Top Land or Ring (normalized)
F	Maximum Face Width (in)
T_1	Maximum Operating Input Torque (in-lbs)
ω_1	Maximum Operating Input Speed (rpm)
Q	Manufacturing Gear Class [7]
N_p	Number of Desired Planet Gears
K_o	Overload Factor
GR	Desired Gear Ratio of SPGS
ϕ_n	Standard Normal Pressure Angle (deg)
Δs_{n1}	Amount Sun Gear Tooth is Thinned for Backlash (normalized)
Δs_{n2}	Amount Sun Gear Tooth is Thinned for Backlash (normalized)
Δs_{n3}	Amount Sun Gear Tooth is Thinned for Backlash (normalized)
ρ_{ao1}	Tool Tip Radius Sun Gear (normalized)
ρ_{ao2}	Tool Tip Radius Planet Gear (normalized)
ρ_{ao3}	Tool Tip Radius Ring Gear (normalized)

TABLE 3. Continued

δ_{ao1}	Effective Tool Protuberance Sun Gear (Normalized)
δ_{ao2}	Effective Tool Protuberance Planet Gear (Normalized)
δ_{ao3}	Effective Tool Protuberance Ring Gear (Normalized)
n_{c1}	Tool Tooth Number Sun Gear
n_{c2}	Tool Tooth Number Planet Gear
n_{c3}	Tool Tooth Number Ring Gear
h_{a1}	Addendum Height Sun Gear (normalized)
h_{a2}	Addendum Height Planet Gear (normalized)
h_{a3}	Addendum Height Ring Gear (normalized)
h_{d1}	Dedendum Height Sun Gear (normalized)
h_{d2}	Dedendum Height Planet Gear (normalized)
h_{d3}	Dedendum Height Ring Gear (normalized)
CL_{12}	Clearance Sun to Planet (normalized)
CL_{21}	Clearance Planet to Sun (normalized)
CL_{23}	Clearance Planet to Ring (normalized)
CL_{32}	Clearance Ring to Planet (normalized)
LR_{12}	Minimum Contact Ratio Pinion to Planet
LR_{23}	Minimum Contact Ratio Planet to Ring

It is recommended to use industry standard values as well as tool geometry input based on available tools. However, custom inputs may improve the optimization performance. Material properties are based on the users selection of material, and allowable stresses. For cycles under material endurance limit, allowable stresses may be based on a damage analysis and S-N (stress vs. cycle data) data with a user defined reliability factor on life.

The outer most block of calculations is an iteration algorithm called the top-level optimization block. The top-level optimization block is a loop is responsible for

calculating the gear ratio, verifying constraints, running the geometry factor optimization block, the pitch diameter optimization block, and the face width optimization block. This block stores the results for each tooth count combination for the users evaluation. The block diagram for the top-level optimization is shown below in Figure 11.

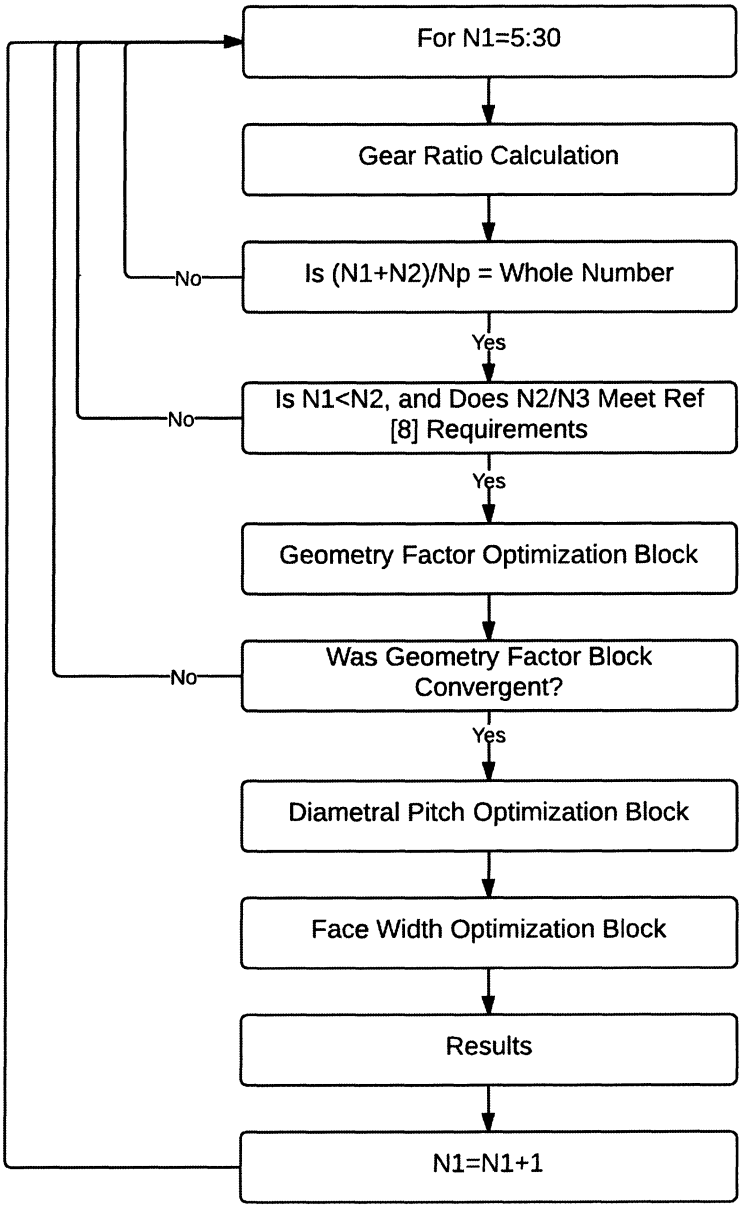

FIGURE 11. Top-level optimization block diagram.

The top-level optimization block starts by assigning 5 teeth to the sun gear. Upon completion of the block or at any point the gear combination is rejected, the block is stopped and reset back to the start where it continues with the next tooth count up to a tooth count of 30 on the sun. The reason for selecting this range of tooth count is any number of teeth below 5 for a sun gear is typically not geometrically possible. In addition, there is infrequently any use for a sun gear with a tooth count greater than 30. This of course is optional and can be tailored to the needs of the designer.

The first action in the top-level block is to calculate the ring and planet number of teeth, and subsequently the gear ratio. Using the input gear ratio provided as a minimum requirement, and rounding up to the nearest ring gear tooth count (using the gear ratio equation for a SPGS) accomplishes this first action. Note: recall that this procedure is tailored for a SPGS with input in the sun gear and output at the carrier. Minor code changes can adjust this function.

The number of teeth on the ring are found by rounding up:

$$N3 = N1 * (GR - 1) \quad \text{.....Equation 1}$$

The number of teeth on the planet are found by rounding down:

$$N2 = \frac{(N3-N1)}{2} - 1 \quad \text{.....Equation 2}$$

Note that the equation for the planet gear subtracts one tooth from the exact solution, and is then round down. This is done to provide room for the planet gear to move between the sun and the ring, giving freedom to modify the operating center distance. This allows the planet and sun gears to be adjusted later on in order to change gear tooth thicknesses and optimize for bending geometry coefficients.

The resulting actual gear ratio is:

$$GR_a = \frac{N3}{N1} + 1 \quad \text{.....Equation 3}$$

The assembly check block and gear ratio check block verify that the resulting gear geometry calculated can be evenly divided by the selected number of planet gears, and that the size constraints for the individual gears are met. The size constraints are the planet gear must be equal to or larger than the pinion, and the planet to ring gear ratio meets requirements such that there is not interference between the planet and the ring. These requirements vary depending on the size number of teeth and are fully defined in Table 4.19 and 4.18 of [8]. This prevents interference and ensures axial assembly. It is possible to modify the gear code to accommodate planet gears that are both smaller and larger than pinion gears, however the designer must be aware of the geometry factor standards before doing so (AGMA 908-B89).

The geometry factor optimization block shown in Figure 9 above maximizes J1, J2, and I12. This is done while maintaining a ratio of J1 to J2 that is proportional to the allowable stresses of the sun and planet. In addition, the addendums of the sun and planet as well as the dedendum of the ring are modified to increase J1, J2, and J3. The addendum and dedendum portion of the optimization has a less significant impact to the design of the SPGS and also requires custom tooling beyond the designer's original intent (algorithm inputs) to make the gear geometry. It is up to the designer to decide if it makes sense to apply this portion of the geometry optimization.

Once the geometry optimization block is complete the SPGS is verified for convergence. Convergence satisfies that the SPGS meets clearance requirements, no teeth are undercut, and that the top lands of all teeth are larger than minimum requirement. If the geometry optimization block determines the SPGS to be divergent,

the top-level optimization block loops back to the start and continues with the next gear combination.

The first step in the geometry optimization block is to check for an initial run. If it is the first loop for the block the algorithm cannot determine the J1 to J2 ratio and thus cannot adjust for it. After the first loop of the block is complete, the J1 to J2 ratio value has been calculated and can be compared to the sun and planet allowable stress ratio. The goal of this step is to equate the J1 to J2 ratio and stress ratio such that:

$$\frac{J_1}{J_2} = \frac{\sigma_{b2,all}}{\sigma_{b1,all}} \quad \text{.....Equation 4}$$

This permits the gear (between sun and planet) with the larger allowable stress to have higher operating stress. Thinning the tooth that has higher allowable stress and thickening the mating tooth accomplishes this task.

Tooth thinning and thickening is achieved by slightly adjusting the addendum modification coefficient (ref AGMA 908-B89). The addendum modification coefficient adjustment should be equal to the center distance adjustment, as well as equal and opposite in direction for the pinion and planet gear. For example, if the center distance loop adds .001 (normalized) to the center distance each loop, then the addendum modification coefficient adjustment should be modified by .001 on the tooth being thinned, and -.001 on the tooth being thickened. The logic is set up such that the addendum modification coefficient is always adjusted towards the target ratio. This action is executed in the J1 to J2 ratio adjustment block during each center distance loop iteration. The J1 to J2 ratio block is shown below in Figure 12.

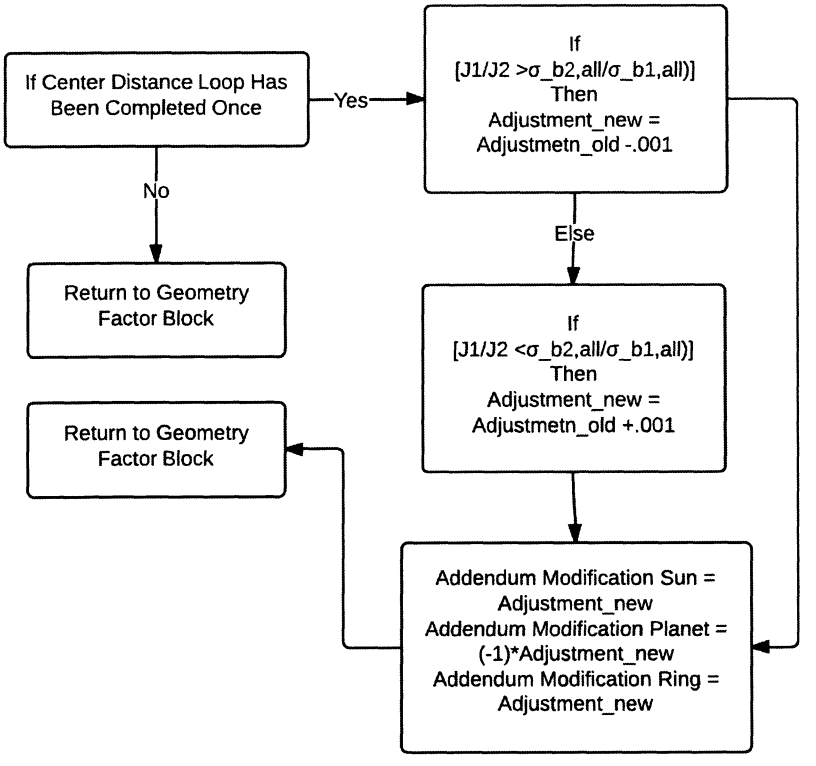

FIGURE 12. J1 to J2 ratio block diagram.

Note that J2 refers to the bending geometry coefficient of the planet, while in contact with the sun. The bending geometry coefficient of the planet while in contact with the ring is typically larger than when in contact with the sun as a result of the ring having both a larger number of teeth and being internal (i.e. J2 on sun < J2 on ring). Therefore it is recommended that only J2 from the planet to the sun be used for stress calculations as a more simple and conservative approach. If desired the designer can set up the algorithm to check both values of J2 and used the largest of the two.

The next step in the geometry optimization block is to calculate J1, J2, and I12. These geometry factors are calculated using American Gear Manufacturers Association (AGMA) 908-B89 information sheet. The geometry factor optimization block

determines J1, J2, and I12 for each value of center distance assigned during the center distance loop. The center distance initial condition is the standard center distance between the sun and the planet (center distance required to locate the gears such that the sun and planet standard pitch diameters are in mesh). Because the planet has at least 1 tooth removed from the standard tooth count, this initial condition for center distance provides room for the planet to be moved away from the sun and towards the ring. As the planet gear moves away from the sun and towards the ring, the planet and sun teeth must become thicker to maintain the desired backlash. The backlash adjustment block diagram is shown below in Figure 13. This results in J1, J2, and I12 to increase, as the planet gear is located further away from the sun via center distance adjustment. The goal of this portion of the optimization is then to increase the J1, J2, and I12 as much as possible while maintaining the necessary and desired geometry constraints.

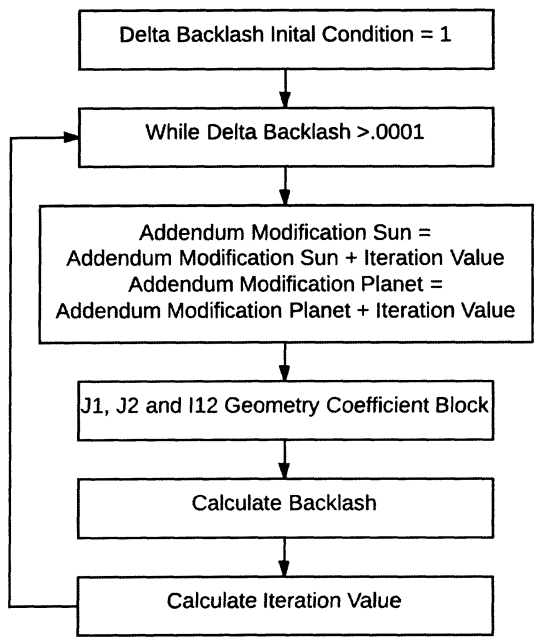

FIGURE 13. Backlash adjustment block.

For each iteration loop the geometry factors must be re-calculated. Because the center distance between the sun and planet are not standard, the addendum modification coefficients must be adjusted to thicken the teeth of the gears. The extent of the gear tooth thickening is determined by adjusting the thickness until the desired backlash is attained. After the first center distance iteration, and new operating pitch diameters have been established, the new backlash value must be calculated and subsequently adjusted to return backlash to the desired requirement. This is done by first creating an iteration value of the addendum modification coefficient based on the approximate difference between actual backlash and required backlash. The iteration value is:

$$x_{1itr} = x_{2itr} = \frac{\frac{d_1 * \pi}{N_1} - s_{n1op} - s_{n2op} - (\Delta_{sn1} + \Delta_{sn1})}{4 * \tan \phi} \quad \text{.....Equation 5}$$

The iteration value variables are listed below in Table 4:

TABLE 4. Iteration Value Variables

x_{1itr}	Addendum Modification Coefficient Iteration Value Sun
x_{2itr}	Addendum Modification Coefficient Iteration Value Planet
d_1	Operating Pitch Diameter Sun
s_{n1op}	Tooth Thickness at Operating Pitch Diameter Sun
s_{n2op}	Tooth Thickness at Operating Pitch Diameter Sun
ϕ	Standard Transverse Pressure Angle

Note that the operating tooth thicknesses (at the operating pitch diameters) are not derived in the AGMA 908-B89 information sheet. For that reason the angles used to

calculate the tooth thicknesses are derived in this thesis along with top land angles. These derivations are found in Appendix A and B.

The addendum modification coefficient iteration value is added symmetrically to the addendum modification coefficient for both the pinion and the planet. J1, J2, and I12 are then re-calculated and the process is looped until the difference between calculated backlash and required backlash are within desired error bounds. The difference between calculated backlash and required backlash is:

$$\Delta_{backlash} = ABS\left[\frac{d_1 * \pi}{N1} - s_{n1op} - s_{n2op} - (\Delta_{sn1} + \Delta_{sn1})\right] \text{.....Equation 6}$$

The values used to modify the addendum modification coefficients are equal and thus adjust the tooth thicknesses symmetrically. The J1 to J2 ratio adjustment covered earlier is separate and covers the non-symmetric tooth thickness of the J1 to J2 ratio independently.

The backlash loop is repeated independently for J3 and I23. This is done because there is no internal bending geometry factor information available in AGMA 908-B89. Therefore the internal bending geometry factor must either be derived or estimated. Because the derivation of J3 is beyond the scope of this document, estimation was used to define it. This estimation assumes that the planet to ring mesh is external and then multiplies the resulting J3 by an empirically derived modification factor. The empirical J3 factor was derived/defined in reference [9]. The J3 modification factor is:

$$J_{3factor} = \left[1 + \frac{3}{N3}\right] \text{.....Equation 7 [9]}$$

Where:

$$N3 = Number\ of\ Teeth\ on\ Ring \text{ .....Equation 8}$$

After the completion of the geometry factor solutions, the center distance is increased and the loop is executed again. This continues until the geometric constraints are almost exceeded/approached to a predefined tolerance. These constraints are listed below in Table 5:

Table 5. Center Distance Loop Geometric Constraints

CL_{12}	Clearance Sun to Planet (normalized)
CL_{21}	Clearance Planet to Sun (normalized)
CL_{23}	Clearance Planet to Ring (normalized)
CL_{32}	Clearance Ring to Planet (normalized)
TL_1	Clearance Sun to Planet (normalized)
TL_2	Minimum Top Land or Planet (normalized)
TL_3	Minimum Top Land or Ring (normalized)

At the start of the center distance iteration loop all clearances are at a maximum. This is a result of the center distance initial condition being equal to the standard center distance between the sun and the planet. As the center distance is incrementally increased the planet moves away from the sun and towards the gear, causing the sun to planet clearances and the planet to ring clearances to decrease. In addition, the top land for the pinion and planet decrease.

As the center distance is increased J1 and J2 are also increased (and concurrently ratio adjusted by the ratio adjustment block) while J3 and I23 are decreased. Since the objective of the center distance iteration loop is to maximize J1, J2, and I12, the center distance continues to be increased until limited by either the clearance or the top land constraints. If desired, an additional constraint can be added to limit the decrease J3 and I23.

Undercutting of the sun and planet as well as the top land for the ring are also geometrically limiting constraints of the gear set. As center distance in increased however, undercutting in the pinion and planet is decreased while the top land on the ring is increased. Therefore, these constraints should not be used during the iteration process. Rather, they are a means to determine whether the SPGS geometry converges or diverges. At the completion of the center distance iteration loop the sun and planet are checked for undercutting and the ring is checked for top land. If the sun or planet is undercut, or if the ring top land is too small, then the SPGS geometry was divergent and does not have a viable solution. If the geometry factor optimization block outputs a divergent SPGS, then the top-level optimization block is stopped and reset at the start for the next gear tooth combination (see Figure 11).

The final actions of the geometry optimization block are to modify the sun and planet addendums as well as the ring dedendum. These optimizations do not affect the operating tooth thickness for any gear. They only affect the addendum and dedendum of the teeth. Because this optimization refines the initial input values for these features, the designer must decide if this level of custom gearing is necessary or beneficial. The Addendum modification block diagram for the sun is shown in Figure 14. The planet addendum modification block diagram and ring dedendum block diagram are similar to Figure 14, with exception to the addendum/dedendum being modified and the applied constraints.

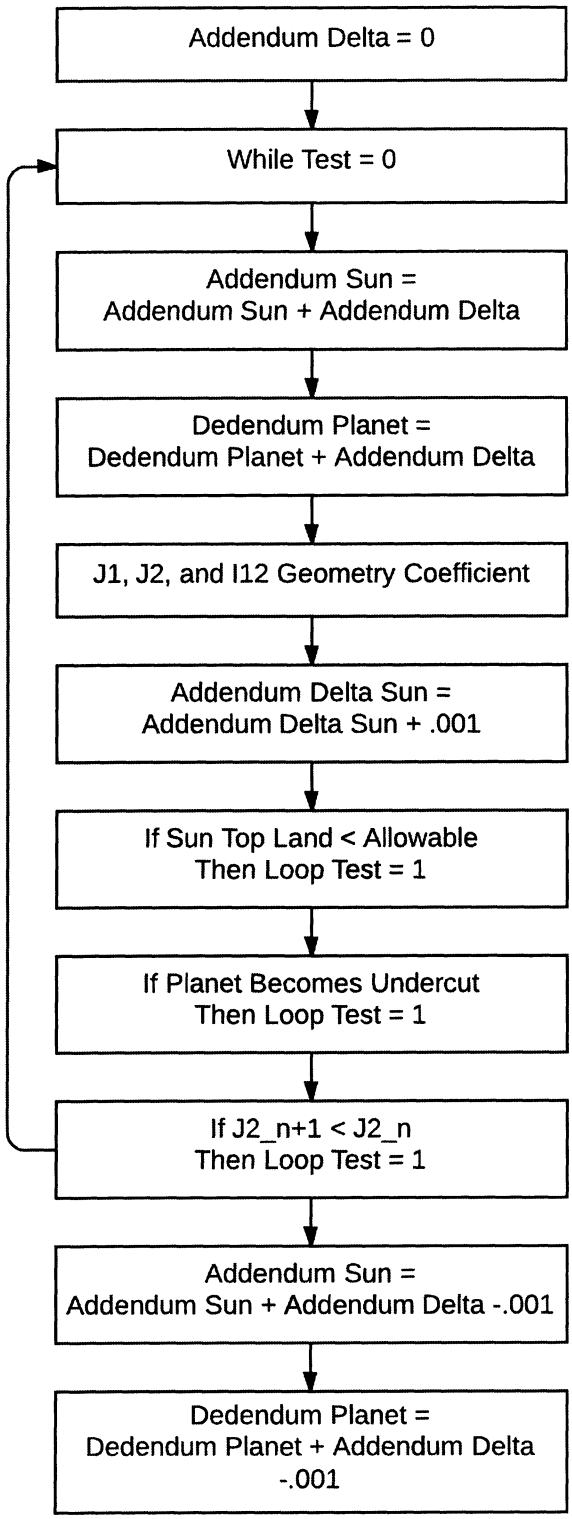

FIGURE 14. Addendum modification block diagram.

The addendum modification loop on the sun increases the addendum of the sun and subsequently increases the dedendum of the planet. This causes J2 to increase as a result of the height of the Lewis parabola, the critical thickness of the tooth, and the radius of curvature at the tooth fillet (See Figure 2 and Figure 15 below). As the dedendum of the planet is decreased, the height of the Lewis parabola increases and the critical thickness of the tooth may either increase of decrease. The addendum modification loop continues to increase the addendum of the sun until either the top land of the sun exceeds the allowable limit, the planet becomes undercut, or if J2 decreases in value. Typically J2 will increase, however it should verified during the modification loop. If any of these limits are exceeded, the loop is terminated and the addendum is reset to the previous valid solution.

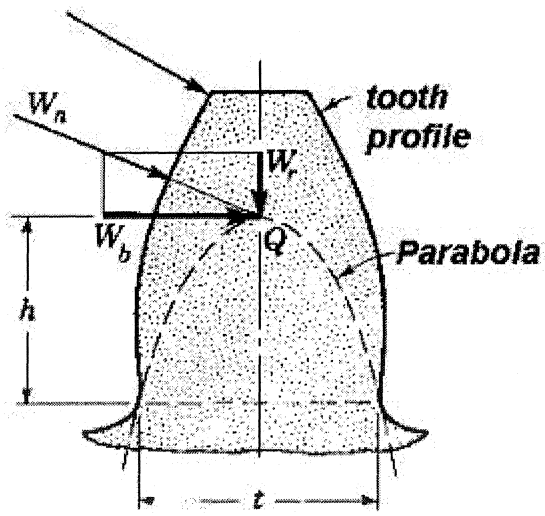

FIGURE 15. Lewis parabola in tooth cross section [16].

The addendum modification loop on the planet decreases the addendum of the planet while subsequently decreasing the dedendum of the sun. This causes J1 to

increase as a result of the height of the Lewis parabola, the critical thickness of the tooth, and the radius of curvature at the tooth fillet. However, in this case both the contact ratios (sun to planet and planet to ring) and J3 decrease. Therefore, if it is desired that J3 be limited on the amount it reduces, this needs to be added as a constraint in the loop. In addition, because of the different geometry variations, J1 will either increase a limited amount and then began to decrease, or never increase at all.

Thus the constraints used for the planet addendum modification loop are the contact ratio between the sun and the planet and the contact ratio between the planet and ring. Also J1 must always be increasing. Because the addendum of the planet and dedendum of the sun are decreasing there is no need to check the top land of the planet or undercutting for the sun. If any of the constraints are exceeded the loop is stopped and the planet addendum is returned to the previous valid solution.

The dedendum modification loop for the ring gear decreases the ring dedendum only. This causes J3 to increase as a result of the height of the Lewis parabola, the critical thickness of the tooth, and the radius of curvature at the tooth fillet. The contact ratio is not affected. Because only the dedendum of the ring is being modified, only the clearance between the planet and the ring needs to be used as limiting constraint along with a verification that J3 is always increasing.

The final optimization steps for the top-level optimization block are the diametral pitch and face with optimization blocks. The diametral pitch and face width optimization blocks are shown below in Figures 16 and 17.

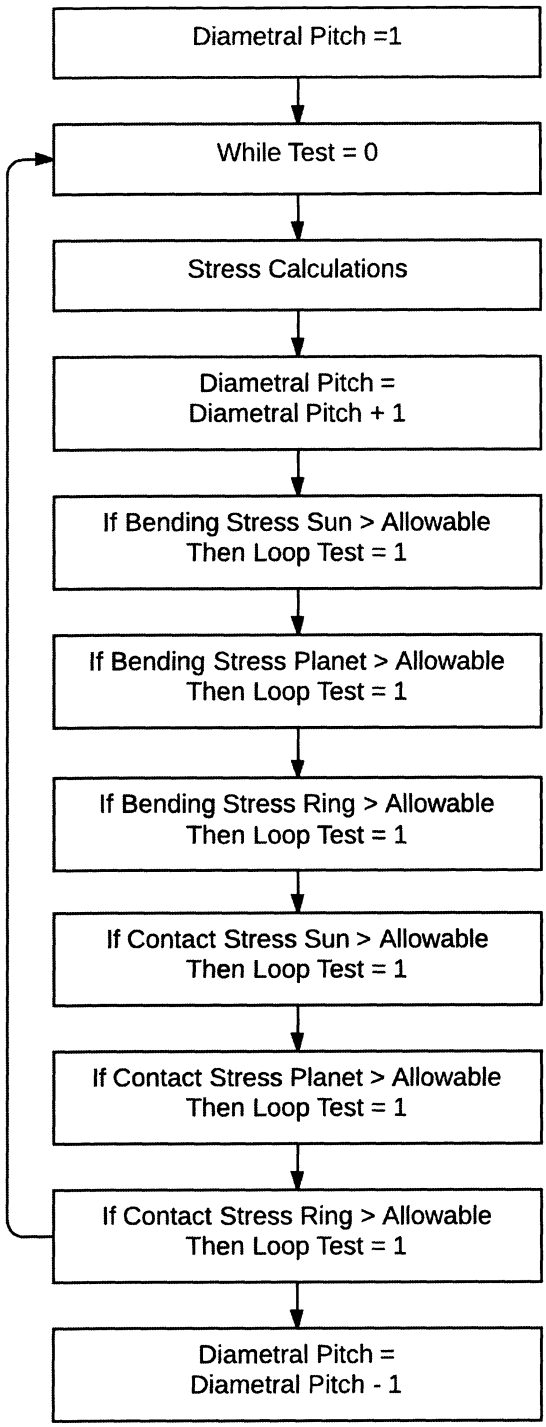

FIGURE 16. Diametral pitch block diagram.

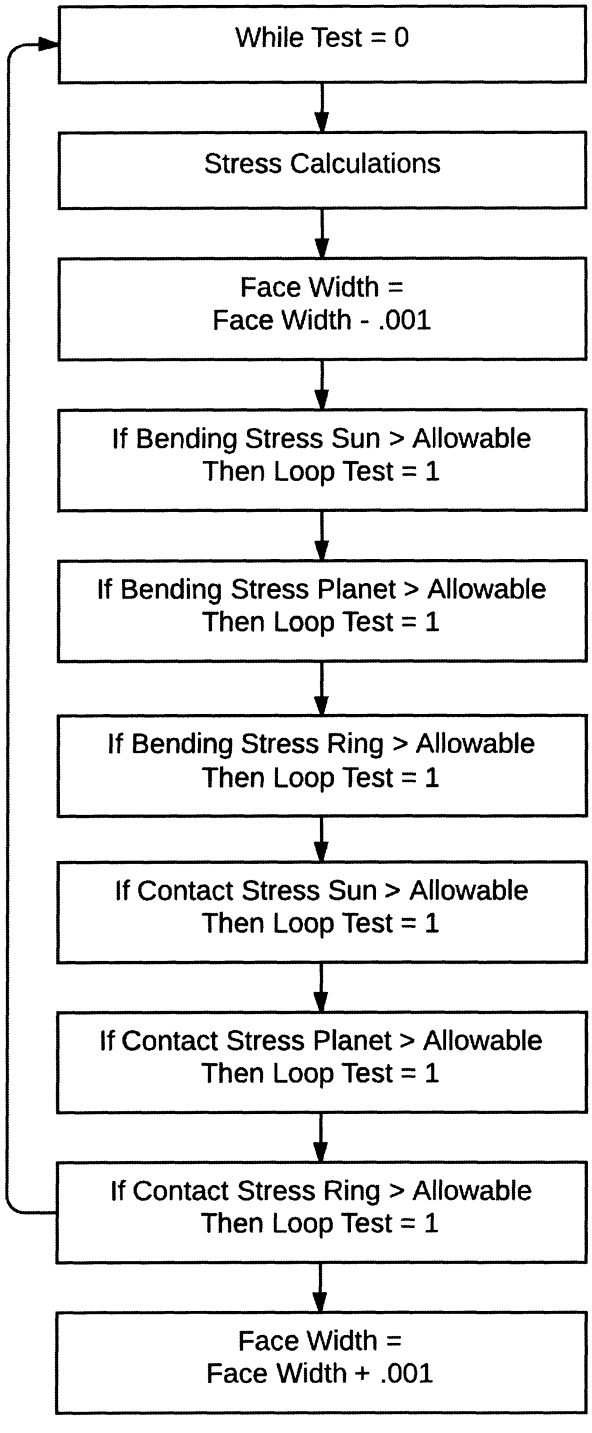

FIGURE 17. Face width block diagram.

The diametral pitch and face width blocks are both stress loops that minimize the outer diameter of the SPGS and the face width. The geometry used in both of these loops is the flowed down optimized geometry for each viable gear tooth combination. Because the face width has been defined as a maximum value requirement, the diametral pitch loop runs first using this required value as the face width. Subsequently, the face with loop runs and minimizes the face with further within the bounds of the constraints.

The diametral pitch and face width optimizations are based on AGMA stress equations for bending and contact stress (listed in Background).

The diametral pitch optimization loop begins with a course pitch equal to 1. For each loop both bending and contact stress is calculated for all 3 gears in the SPGS. Each loop increases the diametral pitch until one of the bending or contact stresses is exceeded. When the loop is completed the diametral pitch is set to the previous value that most recently resulted in the stress being below the allowable provided requirement. Because the designer may want to use rational values for the diametral pitch iterations, it is suggested that the loop integer be assigned to a predetermined diametral pitch matrix. The corresponding diametral pitch may then be used for the stress calculations.

The face width optimization loop begins with the face width set to the maximum allowed requirement provided. For each loop both bending and contact stress is calculated for all 3 gears in the SPGS. Each loop decreases the face width by a small increment until one of the bending or contact stresses is exceeded. When the loop is completed the face width is set to the previous value that most recently resulted in the stress being below the allowable provided requirement.

At the completion of the top-level optimization loop the results of the SPGS are stored for later evaluation. The top-level loop is then run again for the next gear tooth combination.

CHAPTER 4

RESULTS

Example 1

In the first example the material properties for the sun, planet, and ring have been chosen in anticipation of the larger values for J3 and I23 generally realized on the ring. Therefore the ring material properties represent a material with less allowable tensile and contact strength then the sun and the planet. This enables the possibility of reducing cost for the SPGS. All of the inputs for this example are listed below in Table 6. The remaining inputs are base on industry standards, available tool geometry, or designer preference.

TABLE 6. Input Data for SPGS Optimization Example Number 1

Input	Sun	Planet	Ring
Allowable Bending Stress (psi)	110000	100000	85000
Allowable Contact Stress (psi)	334000	334000	134000
Poisson's Ratio	0.33	0.33	0.33
Modulus of Elasticity (psi)	29000000	29000000	29000000
Crown	No	Yes	No
Max Operating Torque at Input (in-lbs)	453		
Max Input Speed (rpm)	171		
Manufacturing Gear Class	7		
Number of Planets	3		
Overload Factor	1.30		
Desired Gear Ratio	4.60		
Standard Normal Pressure Angle (degrees)	20		

TABLE 6. Continued

Tooth Thinning for Backlash (normalized)	0.025	0.025	0.025
Tool Tip Radius (normalized)	0.250	0.250	0.250
Tool Protuberance (normalized)	0.000	0.000	0.000
Tool Tooth Number*	1000	1000	1000
Addendum (normalized)	1.00	1.00	1.00
Dedendum (normalized)	1.24	1.24	1.24
Clearance Pinion to Planet	0.150		
Clearance Planet to Pinion	0.150		
Clearance Planet to Ring	0.250		
Clearance Ring to Planet	0.250		
Minimum Contact Ratio Pinion to Planet	1.200		
Minimum Contact Ratio Planet to Ring	1.200		
Minimum Top Land*	0.400	0.400	0.250

* Tool tooth number of 1000 indicates use of a rack or hob tool cutter. For internal gears the tool tooth number must be less than the number of teeth on the ring. This example uses a rack or hob because the bending geometry factor is a modified external gear mesh factor. * Top land for the sun and the planet is larger than that of the ring because these gear properties reflect carburized material and need resistance to brittle chipping at the tooth tip.

This example ran all possible gear combinations with the sun ranging from 5 to 30 teeth. The resulting solutions that met all design criteria and were convergent solutions are listed below in Table 7.

TABLE 7. Basic SPGS Characteristics for Example 1 Results

Solution Number	Gear Ratio	Diametral Pitch (teeth/in)	Number Teeth Sun	Number Teeth Planet	Number Teeth Ring	Face Width (in)
1	4.615	14	13	16	47	0.400
2	4.600	18	15	18	54	0.359
3	4.636	27	22	28	80	0.377
4	4.625	31	24	30	87	0.387
5	4.615	32	26	33	94	0.381
6	4.607	34	28	35	101	0.383
7	4.600	36	30	38	108	0.394

The resulting bending and contact stresses are listed below in Table 8. The bending stress of the planet gear was based on the bending geometry factor of the planet when in mesh with the sun. Generally this is a conservative approach since J2 in mesh with the sun is less than J2 mesh with the ring. The stress can be evaluated for both meshes and the higher of the two used if desired.

The volume of the SPGS is based on the outer diameter and face width of the gear set. This is a rough estimation and can be calculated more accurately if desired. The smallest volume SPGS is estimated to be the lightest option. Note that the planet size, bearing size, and techniques to lighten gears are not accounted for in this volume estimate.

TABLE 8. SPGS Stress and Volume Results for Example 1

Solution Number	Bending Stress Pinion (psi)	Bending Stress Planet (psi)	Bending Stress Ring (psi)	Contact Stress Pinion to Planet (psi)	Contact Stress Planet to Ring (psi)	Volume (in^3)
1	39740	36860	32970	232840	133870	5.98
2	60450	55180	49740	268640	133960	3.94
3	79320	70630	70370	262260	133960	3.83
4	91840	81430	82160	273490	133920	3.36
5	89850	79170	81370	261890	133890	3.63
6	92290	80960	84830	258470	127690	3.58
7	95560	80790	84900	251760	128800	3.77

Through the data shown in Table 8 and the volume data plotted below in Figure 18 below it is clear that the smallest and lightest SPGS option is solution number 4. The limiting factor for this set was the contact stress on the ring, which finished at 133920 psi

and had an allowable of 134000 psi. In fact, all solutions were limited by either the ring contact stress or bending stress.

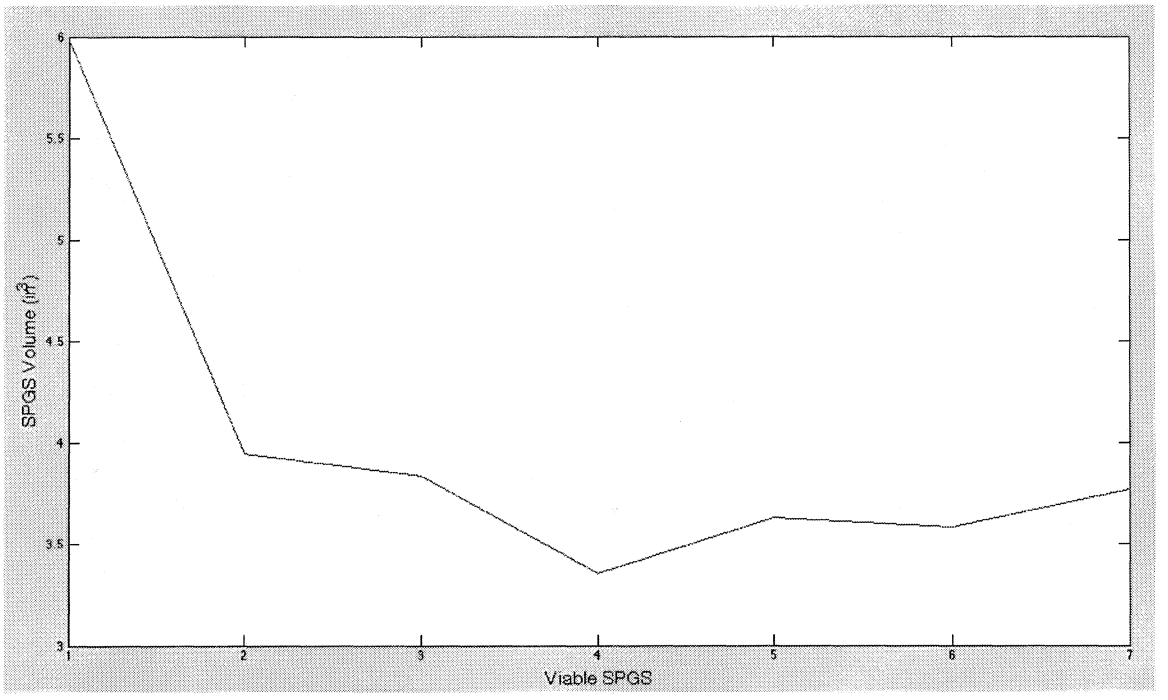

FIGURE 18. SPGS volume plotted vs. solution number for example 1.

For solution number 4, the center distance iteration data is shown below in Figure 19. Here the bending geometry factor for the sun, planet, and ring is plotted against the iteration number. The bending geometry factor for the sun is shown in blue, planet in green, and the ring in red. During approximately the first 50 iterations, the bending geometry factor for the sun and planet move away from each other and the ring decreases at a similar rate. This is a result of the J1 to J2 ratio being achieved. Once the J1 to J2 ratio is achieved, both J1 and J2 factors increase at the same rate. J3 is decreasing during the optimization as a result of the ring gear teeth becoming thinner as the planet is moved

away from the sun and closer to the ring. If the ring gear bending stress becomes a limiting design factor, the designer can choose to limit the center distance optimization based on the J3 value with respect to J1 and or J2.

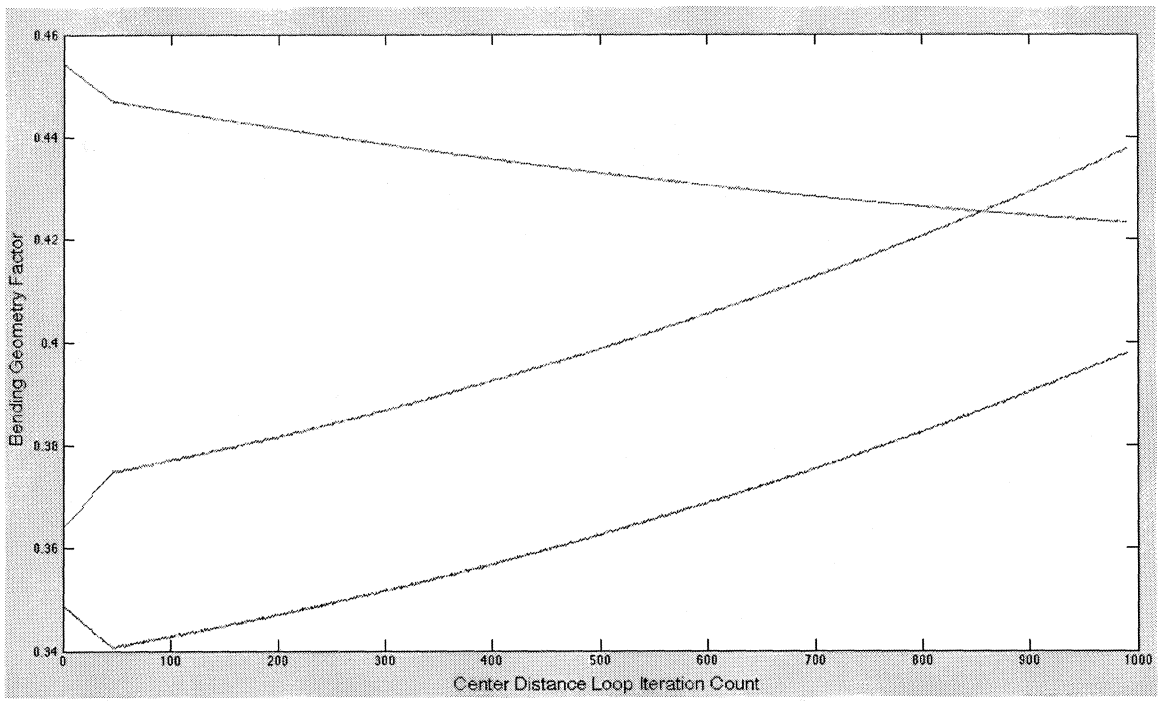

FIGURE 19. Bending geometry factors vs. center distance loop iteration count for example 1 solution number 4.

Figure 20 below illustrates I12 and I23 throughout the center distance iteration loop. It is shown by this data that the contact geometry factor usually follows the bending factor. As a result of the planet to ring being an internal mesh I23 is significantly higher than that of I12. For this reason the ring gear contact stress is not a driving factor in the optimization technique. However, because in this case the ring gear was the limiting factor on contact stress, it may appear to be possible to achieve a better

solution for solution numbers 2 and 3 by limiting the center distance iteration loop. This idea is covered in more detail in example 2.

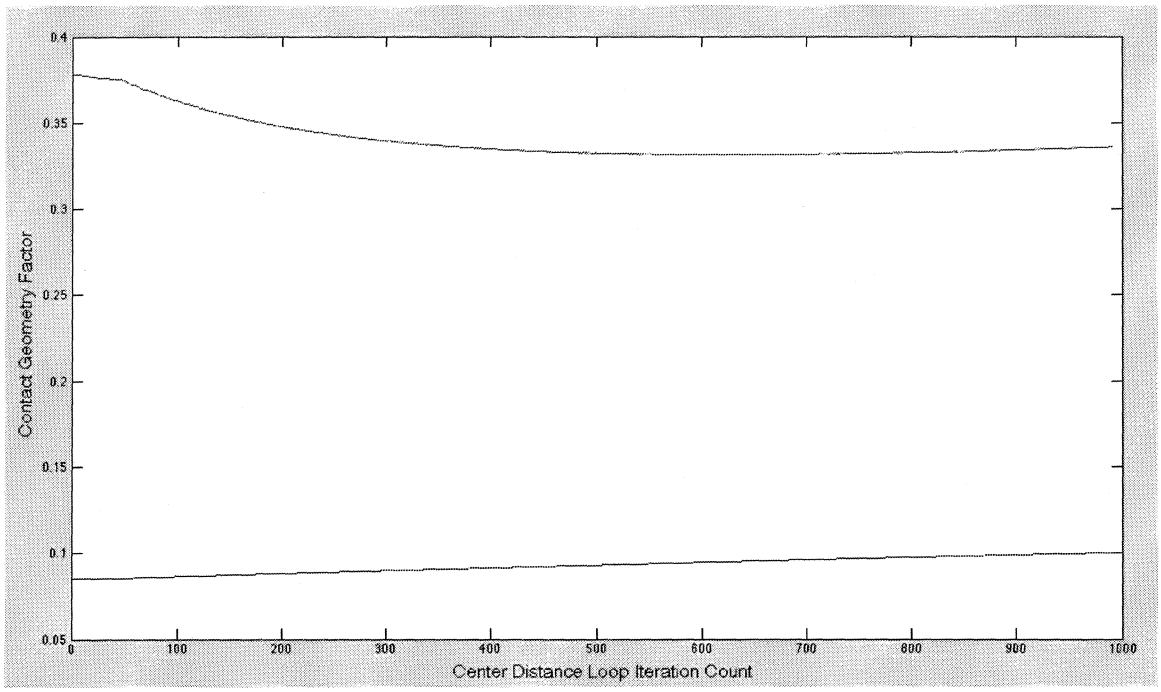

FIGURE 20. Contact geometry factors vs. center distance loop iteration count example 1.

Figure 21 below shows J1, J2, and J3 plotted against the addendum/dedendum modification loop iteration count. J1 is shown in blue, J2 in green, and J3 in red. The sharp decline in data at the termination of J1 and J3 is only the termination of the data and does not reflect the actual geometry factor. The final geometry factors are the highest values prior to loop termination. As seen in the data the J1 factor was not increasing as the planet addendum was decreased. This resulted in the program terminating the loop prior to other constraints causing termination. The J2 and J3 factors

had mild increases as a result of the iteration loop. Again, because this would result in custom tooling, this is a design function the designer must decide is necessary.

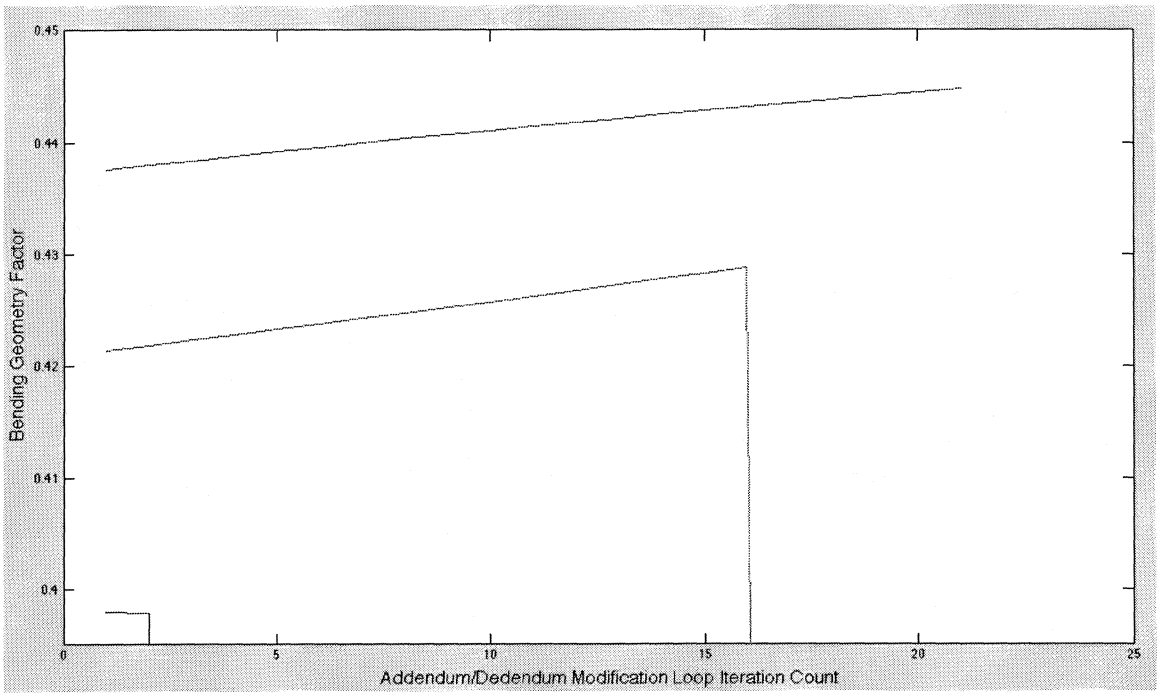

FIGURE 21. Bending geometry factors vs. addendum/dedendum modification loop iteration count example 1.

Because the contact geometry factors did not significantly change during the addendum/dedendum iteration loop, that data has been omitted and considered inconsequential to the results.

Example 2

In this example the material properties for the sun, planet, and ring have been chosen such that they are the same or similar materials. The ring however is not hardened and thus has a lower allowable contact strength. The planet has lower allowable bending strength as a result of the stress ratio being -1. All of the inputs for

this example are listed below in Table 9. The remaining inputs are based on industry standards, available tool geometry, or designer preference.

TABLE 9. Input Data for SPGS Optimization Example Number 2

Input	Sun	Planet	Ring
Allowable Bending Stress (psi)	100000	90000	100000
Allowable Contact Stress (psi)	300000	300000	200000
Poisson's Ratio	0.33	0.33	0.33
Modulus of Elasticity (psi)	29000000	29000000	29000000
Crown	No	Yes	No
Max Operating Torque at Input (in-lbs)	2000		
Max Input Speed (rpm)	140		
Manufacturing Gear Class	7		
Number of Planets	3		
Overload Factor	1.30		
Desired Gear Ratio	6.19		
Standard Normal Pressure Angle (degrees)	2		
Tooth Thinning for Backlash (normalized)	0.025	0.025	0.025
Tool Tip Radius (normalized)	0.250	0.250	0.250
Tool Protuberance (normalized)	0.000	0.000	0.000
Tool Tooth Number*	1000	1000	1000
Addendum (normalized)	1.00	1.00	1.00
Dedendum (normalized)	1.24	1.24	1.24
Clearance Pinion to Planet	0.150		
Clearance Planet to Pinion	0.150		
Clearance Planet to Ring	0.250		
Clearance Ring to Planet	0.250		
Minimum Contact Ratio Pinion to Planet	1.200		
Minimum Contact Ratio Planet to Ring	1.200		
Minimum Top Land*	0.400	0.400	0.250

* Tool tooth number of 1000 indicates use of a rack or hob tool cutter. For internal gears the tool tooth number must be less than the number of teeth on the ring. This example uses a rack or hob because the bending geometry factor is a modified external gear mesh factor. * Top land for the sun and the planet is larger than that of the ring because these gear properties reflect carburized material and need resistance to brittle chipping at the tooth tip.

This example ran all possible gear combinations with the sun ranging from 5 to 30 teeth. The resulting solutions that met all design criteria and were convergent solutions are listed below in Table 10. The Face width results shown in table 10 bring up an important observation. The ratio of the diameter to the width of the gears is high in this gear set (diameter data omitted but can be calculated using number of teeth and diametral pitch). Therefore the designer may desire to run the algorithm again using a larger face width. This points to a logical operation that can be added to the top-level optimization block. As an alternative, the input for the top-level block can be a minimum ratio of diameter to face width for each gear. This would give the optimization process more options for reducing size.

TABLE 10. Basic SPGS Characteristics for Example 2 Results

Solution Number	Gear Ratio	Diametral Pitch (teeth/in)	Number Teeth Sun	Number Teeth Planet	Number Teeth Ring	Face Width (in)
1	6.214	9	14	28	73	0.327
2	6.200	10	15	30	78	0.343
3	6.188	11	16	32	83	0.361
4	6.222	17	27	56	141	0.389
5	6.214	17	28	58	146	0.372
6	6.207	18	29	60	151	0.400
7	6.200	18	30	62	156	0.384

The resulting bending and contact stresses are listed below in Table 11. In this example the ring was never the limiting component of the gear train. Instead, it was the

contact stress between the sun and planet gear, and the bending stress of the sun that was the limiting factor.

TABLE 11. SPGS Stress and Volume Results for Example 2

Solution Number	Bending Stress Pinion	Bending Stress Planet	Bending Stress Ring	Contact Stress Pinion to Planet	Contact Stress Planet to Ring	Volume (in^3)
1	74760	67570	62880	300000	116840	23.90
2	79990	71640	68860	299760	117260	23.10
3	85060	75830	73700	299720	117630	22.51
4	99770	85490	91740	257340	106920	26.78
5	99760	85250	92200	253430	105570	27.28
6	99990	85180	92630	250140	104310	27.80
7	99990	84950	93030	246680	103030	28.32

Through the data shown in Table 11 and the volume data plotted below in Figure 22 below it is clear that the smallest and lightest SPGS option is solution number 3. The limiting factor for this gear set was the contact stress on sun and planet. There was still some excess margin on the bending stress for all 3 gears in the set. Additionally, although the sun and planet have excess margin, the ratio of stress corresponds to the ratio of allowable stress by design. This brings up another important observation. If excess margin is available on bending, then the ratio can be truncated to assist in more efficiently balancing the stresses. This brings a logical operation that can be added a level above the top-level optimization loop: Adjust the J1 to J2 ratio based on top-level block results for further size reduction.

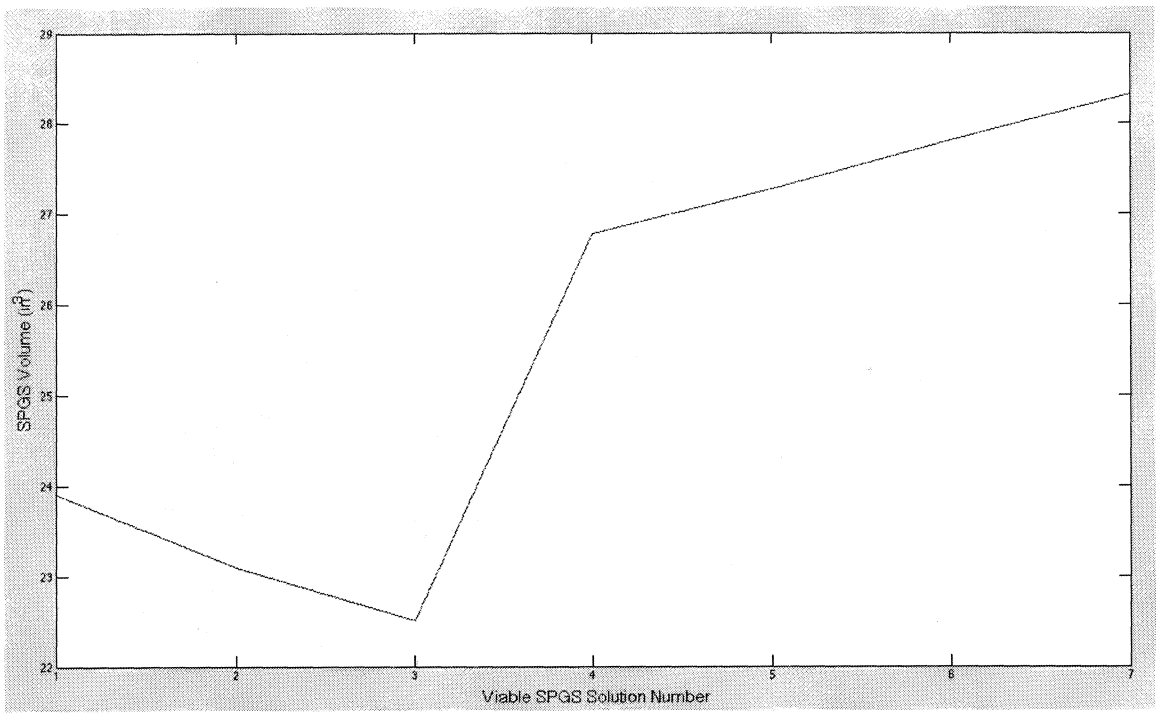

FIGURE 22. SPGS volume plotted vs. solution number example 2.

For solution number 3, the center distance iteration data is shown below in Figure 23. Here the bending geometry factor for the sun, planet, and ring is plotted against the iteration number. The bending geometry factor for the sun is shown in blue, planet in green, and the ring in red. During approximately the first 50 iterations, the bending geometry factor for the sun and planet move toward each other and the ring decreases at a similar rate. This is a result of the J1 to J2 ratio being achieved. Once the J1 to J2 ratio is achieved, both J1 and J2 factors increase at the same rate. J3 is decreasing during the optimization as a result of the ring gear teeth becoming thinner as the planet is moved away from the sun and closer to the ring. If the ring gear bending stress becomes a limiting design factor, the designer can choose to limit the center distance optimization based on the J3 value with respect to J1 and or J2. It would be best to add this additional

constraint along with the J1 to J2 ratio adjustment discussed above. This would allow the algorithm to review the results and then make top-level adjustments.

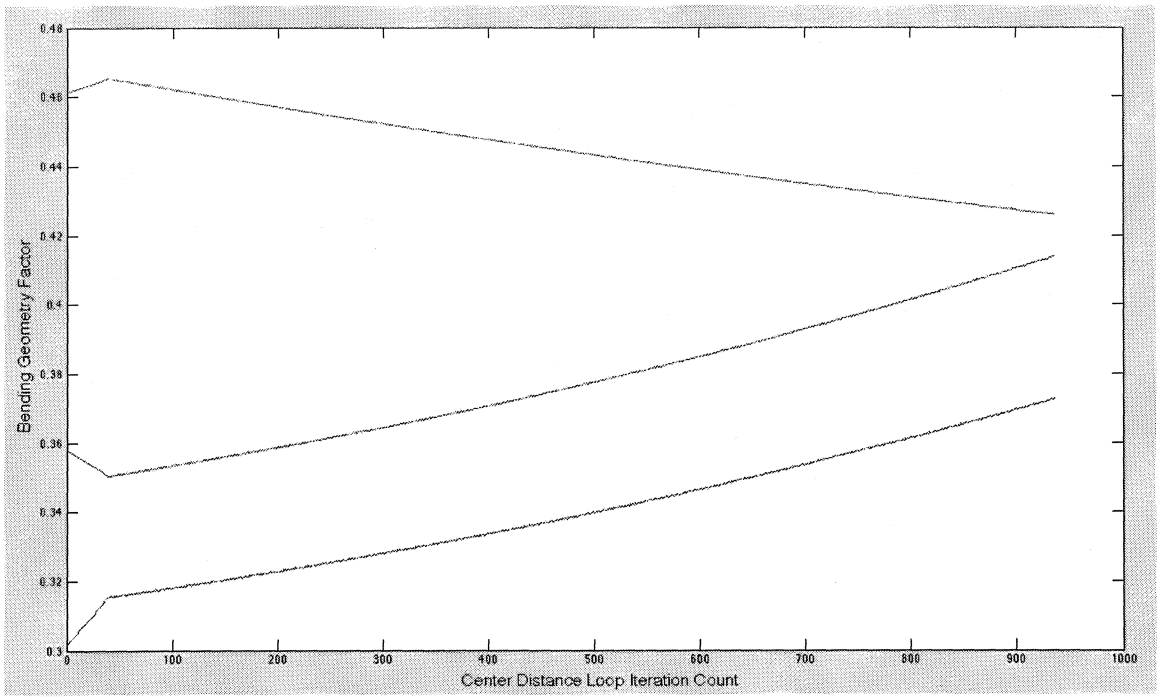

FIGURE 23. Bending geometry factors as a function of center distance loop iteration count for example 2 solution number 4.

Figure 24 below illustrates I12 and I23 throughout the center distance loop iteration count. It is shown by this data that the contact geometry factor usually follows the bending factor. However, in this example I23 reduces exponentially at the start of the iteration. This may lead to the inquiry that the iteration should be terminated early to preserve the large I23 contact factor. First off, the contact stress on the ring is not a driving factor for this gear set. More importantly however this early result of a large contact factor is erroneous. During the first portion of the iteration process the sun and planet have a high probability of being undercut depending on their tooth count.

Concurrently the contact ratio of the planet to ring is low, and the operating pitch diameter of the ring is very close to the base diameter of the ring. All of these aspects would make the early results of the iteration process non-viable results. In this particular case, the ring does not exceed the 1.2 contact ratio requirement, and the sun does not avoid undercutting until I23 decreases to .4 or roughly 350 iterations in. The algorithm is currently set up to move the planet into an area of convergence and terminate prior to the solution becoming divergent.

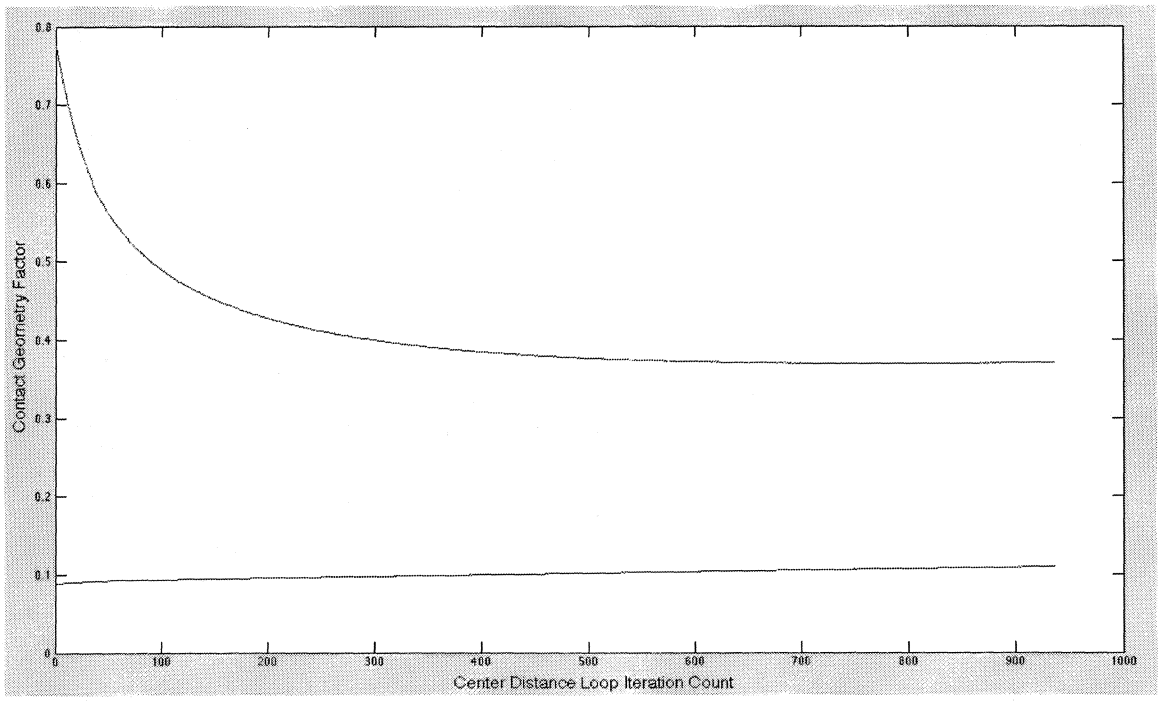

FIGURE 24. Contact geometry factors vs. center distance loop iteration count example 2.

Figure 25 below shows J1, J2, and J3 plotted against the addendum/dedendum modification loop iteration count. J1 is shown in blue, J2 in green, and J3 in red. The sharp decline in data at the termination of J1 and J3 is only the termination of the data

and does not reflect the actual geometry factor. The final geometry factors are the highest values prior to loop termination. In this example J3 starts out lower than J2. This appears erroneous, as these were not the final values after the center distance iteration loop. These results are in fact correct though. The addendum modifications are done sequentially with the sun completed first followed by the planet and the ring. It is understood that when adjusting the planet addendum J3 may be reduced. Because J3 is not typically a limiting factor in the design this was ignored. However, in cases when J3 is a deciding factor, an iteration step can be added to the top-level block that can re-run the optimal result without allowing J3 to be reduced during addendum modification.

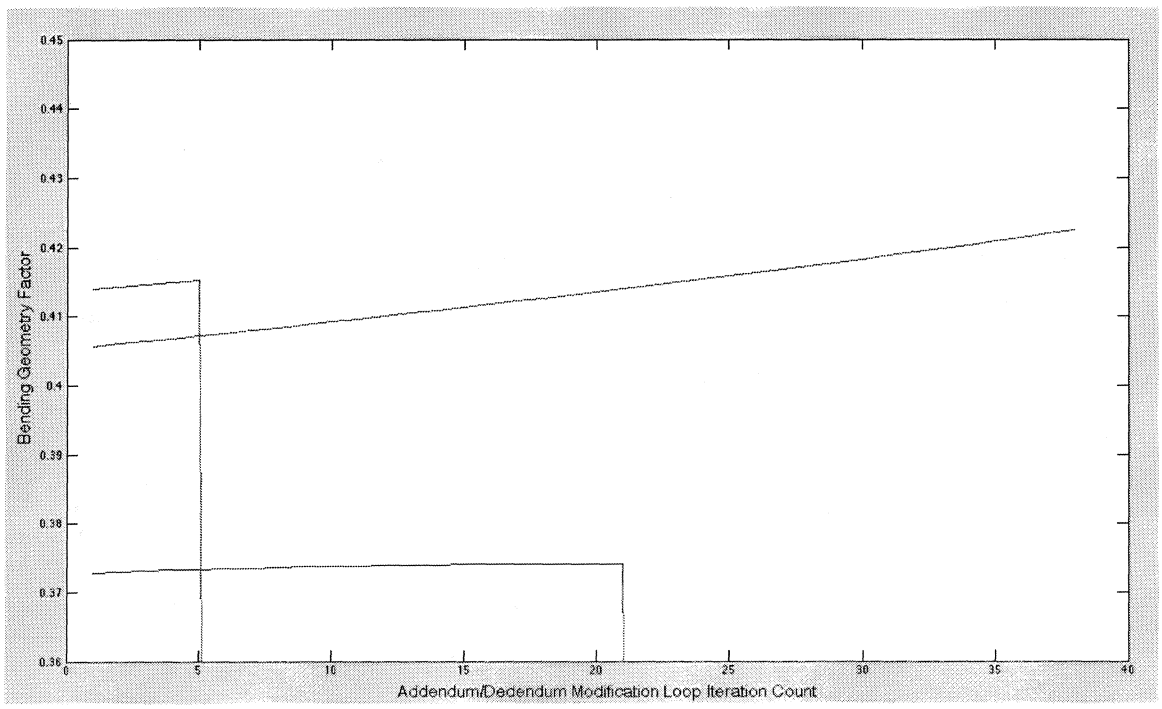

FIGURE 25. Bending geometry factors vs. addendum/dedendum modification loop iteration count example 2.

Because the contact geometry factors did not significantly change during the addendum/dedendum iteration loop, that data has been omitted and considered inconsequential to the results.

CHAPTER 5

CONCLUSION AND FUTURE WORKS

The fundamental approach of the optimization algorithm thoroughly investigates every possible gear tooth geometry combination (number of teeth on the sun) within the desired bounds of the designer. Furthermore, it affectively maximizes the potential of the sun and planet gear by distributing increased stress to the component with higher strength while simultaneously maximizing the strength of both the sun and planet. The algorithm also iterates to find the smallest tooth for each gear tooth combination. This results in the full range of tooth count and size combinations to be verified (small tooth counts with large tooth size, to large tooth counts with small tooth size).

All of the algorithm iterations are completed within the bounds of tooth design limits. Undercutting is prevented, minimum top land is maintained, and desired tooth clearance is preserved. Each solution is also provided with the desired backlash, and the stress equations include all of the necessary design factors. Note: The design factors and values used may be subject to change based on application and individual experience. The resulting gear train is therefore a functional design that must only be checked for fillet root radius clearance and machine tolerances.

Options for improving the optimization algorithm further were identified and presented as additional iteration loops. These suggestions include creating a constraint for a face width to diameter ratio, adding an iteration step to the top-level block for

adjusting the J1 to J2 ratio, and adding an iteration step to the top-level block for limiting the reduction of J3.

For future works this algorithm will be modified to include previously identified optimization improvements. The algorithm will also be formatted to provide a larger range of gear ratios (to allow smaller planet gears), different input and output locations, and gear train efficiency. Finally, this algorithm will be modified to run multiple SPGSs at a time for the use of compound planetary optimization techniques. The inputs of this program have been set up to allow calling by other larger programs that may have larger scopes.

APPENDICES

APPENDIX A

DERIVATION OF TOP LAND AND OPERATING TOOTH THICKNESS ANGLE FOR EXTERNAL GEARS

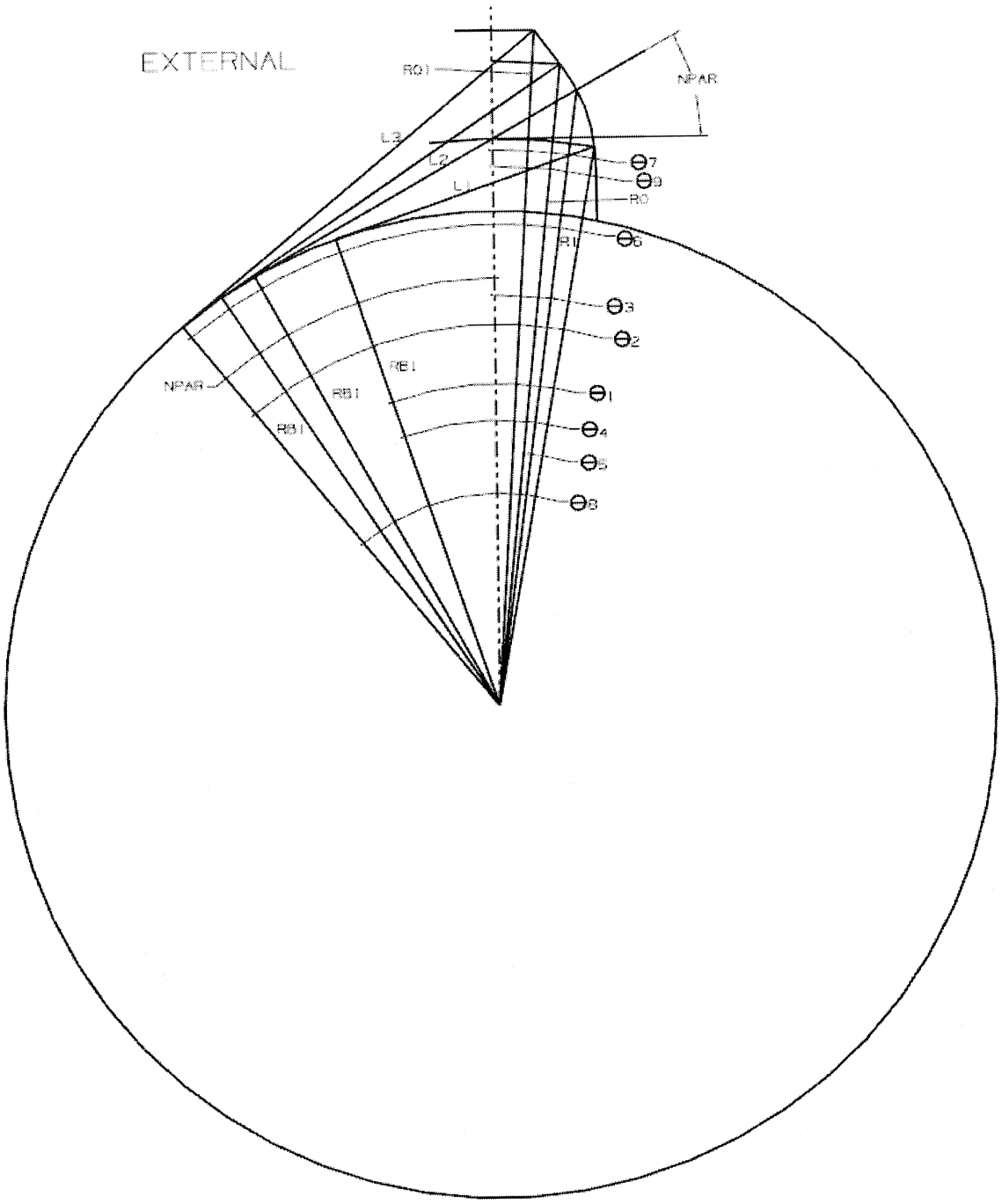
EXTERNAL
RO1
NPAR
L3
L2
L1
θ7
θ9
RO
RI
θ6
θ3
θ2
RB1
NPAR
RB1
RB1
θ1
θ4
θ5
θ8

$$\theta 2 - \theta 3 - \theta 5 = \theta 8$$

$$\theta 7 = \theta 6 - \theta 8$$

$$L3 = RB1 * \theta 2$$

$$RB1^2 + L3^2 = R01^2$$

$$L3 = \sqrt{R01^2 - RB1^2}$$

$$\sqrt{R01^2 - RB1^2} = RB1 * \theta 2$$

$$\theta 2 = \frac{\sqrt{R01^2 - RB1^2}}{RB1}$$

$$\theta 3 = \frac{Sn1}{N1}$$

$$\theta 5 = \theta 1 - \theta 4$$

$$L1 = RB1 * \theta 1$$

$$L1^2 + RB1^2 = R1^2$$

$$L1 = \sqrt{R1^2 - RB1^2}$$

$$\frac{\sqrt{R1^2 - RB1^2}}{RB1} = \theta 1$$

$$\theta 4 = \text{Atan}\left(\frac{L1}{RB1}\right) = Atan\left(\frac{\sqrt{R1^2 - RB1^2}}{RB1}\right) = \theta 4$$

$$\theta 5 = \frac{\sqrt{R1^2 - RB1^2}}{RB1} - Atan\left(\frac{\sqrt{R1^2 - RB1^2}}{RB1}\right)$$

$$\theta 6 = \text{Atan}\left(\frac{L3}{RB1}\right)$$

$$L3^2 + RB1^2 = R01^2$$

$$L3 = \sqrt{R01^2 - RB1^2}$$

$$\theta 6 = Atan\left(\frac{\sqrt{R01^2 - RB1^2}}{RB1}\right)$$

$$\theta 7 = Atan\left(\frac{\sqrt{R01^2 - RB1^2}}{RB1}\right) - \left[\frac{\sqrt{R01^2 - RB1^2}}{RB1} - \frac{Sn1}{N1} - \left(\frac{\sqrt{R1^2 - RB1^2}}{RB1} - Atan\left(\frac{\sqrt{R1^2 - RB1^2}}{RB1}\right)\right)\right]$$

$$\theta 7 = Atan\left(\frac{\sqrt{R01^2 - RB1^2}}{RB1}\right) - \frac{\sqrt{R01^2 - RB1^2}}{RB1} + \frac{Sn1}{N1} + \frac{\sqrt{R1^2 - RB1^2}}{RB1} - Atan\left(\frac{\sqrt{R1^2 - RB1^2}}{RB1}\right)$$

APPENDIX B

DERIVATION OF TOP LAND AND OPERATING TOOTH THICKNESS ANGLE FOR INTERNAL GEARS

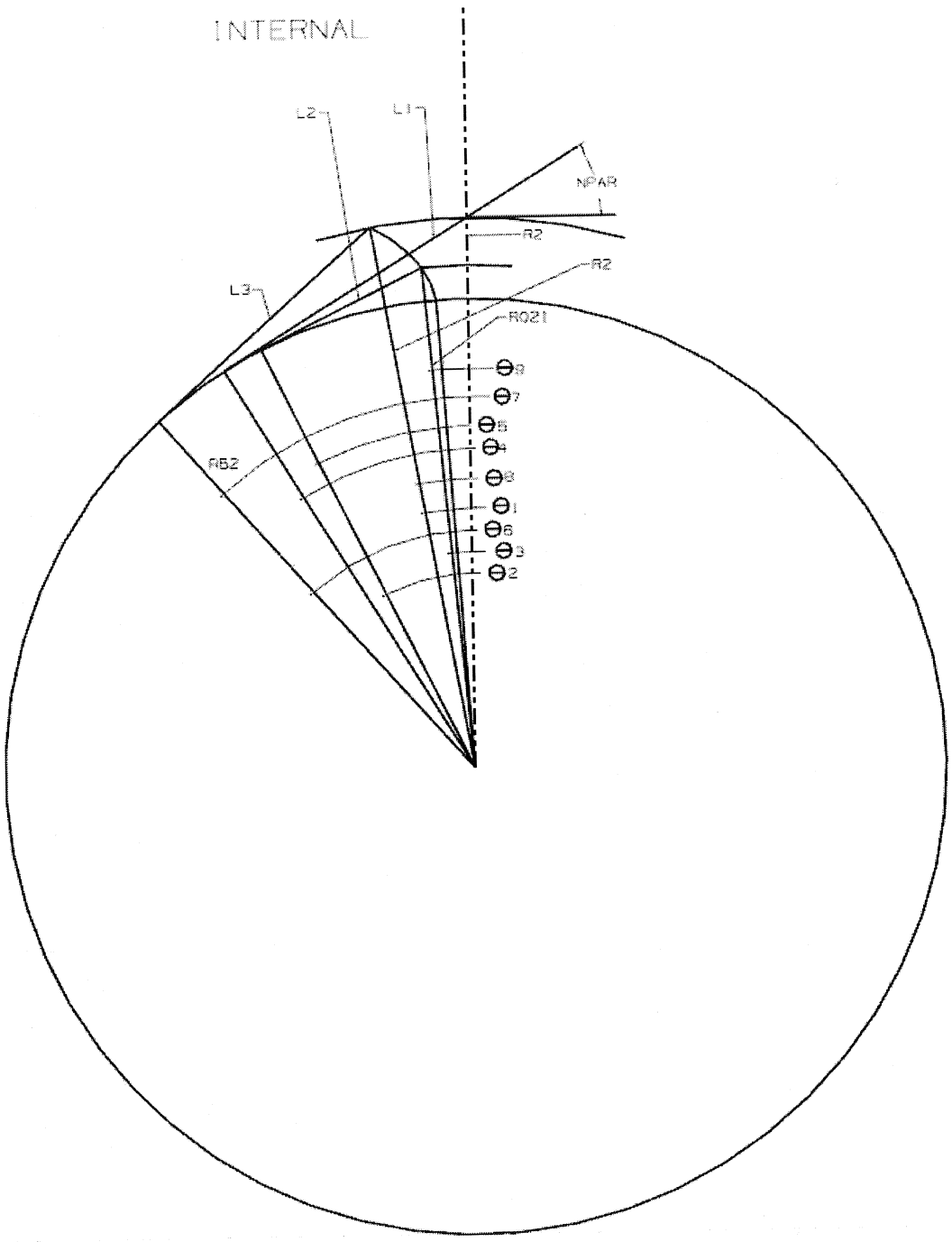
INTERNAL
L2
L1
NPAR
R2
R2
L3
R021
θ9
θ7
θ5
θ4
θ8
θ1
θ6
θ3
θ2
RB2

$$L2^2 + RB2^2 = R02I^2$$

$$L2 = \sqrt{R02I^2 - RB2^2}$$

$$\tan(\theta 2) = \frac{L2}{RB2}$$

$$\theta 2 = \text{Atan}\left(\frac{L2}{RB2}\right)$$

$$\theta 2 = Atan\left(\frac{\sqrt{R02I^2 - RB2^2}}{RB2}\right)$$

$$RB2^2 + L1^2 = R2^2$$

$$L1 = \sqrt{R2^2 - RB2^2}$$

$$\tan(\theta 4) = \frac{L1}{RB2}$$

$$\theta 4 = \text{Atan}\left(\frac{L1}{RB2}\right)$$

$$\theta 4 = Atan\left(\frac{\sqrt{R2^2 - RB2^2}}{RB2}\right)$$

$$\theta 1 = \frac{Sn2}{N2}$$

$$\theta 8 = \theta 7 - \theta 6$$

$$\theta 7\text{: } L3 = RB2 * \theta 7$$

$$L3^2 + RB2^2 = R2^2$$

$$L3 = \sqrt{R2^2 - RB2^2}$$

$$\theta 7 = \frac{\sqrt{R2^2 - RB2^2}}{RB2}$$

$$\theta 6\text{: } \tan(\theta 6) = \frac{L3}{RB2}$$

$$\theta 6 = \text{Atan}\left(\frac{L3}{RB2}\right) = Atan\left(\frac{\sqrt{R2^2 - RB2^2}}{RB2}\right)$$

$$\theta 8 = \frac{\sqrt{R2^2 - RB2^2}}{RB2} - Atan\left(\frac{\sqrt{R2^2 - RB2^2}}{RB2}\right)$$

$$\theta 9 = \theta 5 - \theta 2$$

$$L2 = RB2 * \theta 5$$

$$L2^2 + RB2^2 = R02I^2$$

$$L2 = \sqrt{R02I^2 - RB2^2}$$

$$\theta 5 = \frac{\sqrt{R2^2 - RB2^2}}{RB2}$$

$$\theta 9 = \frac{\sqrt{R2^2 - RB2^0}}{RB2} - Atan\left(\frac{\sqrt{R02I^2 - RB2^2}}{RB2}\right)$$

REFERENCES

REFERENCES

1. Marjanovic, N., Isailovic, B., Marjanovic, V., Milojevic, Z., Blagojevic, M., Bojic, M., 2012, "A practical approach to optimizations of gear trains with spur gears," Mechanism and Machine Theory, **53**, 1-16

2. Wan, Z., Zhang, S., 2013, "Formulation for an optimal design problem of spur gear drive and its global optimization" Proceedings of the Institution of Mechanical Engineers, **227**, 1804-1817

3. Faruk, M., Baskal, T., Boran, K., Boran, F.E., 2010, "Optimization of mudule, shaft diameter and rolling bearing for spur gear through genetic algorithm," Expert Systems with Applications, **37**, 8058-8064

4. Savsani, V., Rao, R.V., Vakharia, D.P., 2010, "Optimal weight design of a gear train using particle swarm optimization and simulated annealing algorithms," Mechanism and Machine Theory, **45**, 531-541

5. Gologlu, C., Zeyveli, M., 2009, "A genetic approach to automate preliminary design of gear drives," Computers and Industrial Engineering, **57**, issue 3, 1043-1051

6. Savage, M., Lattime, S.B., Kimmel, J.A., Coe, H.H., 1994, "Optimal-design of compact spur gear reductions," Journal of Mechanical Design, **116**, 690-696

7. AGMA 390.01

8. Dudley, D. W., and Townsend, D. P., 1992, Dudley's Gear Handbook, 2nd Ed., McGraw-Hill, New York, Chap. 4

9. Singh, A.K., Gangwar, H.P., Saxena, R., Misra, A., 2012, "Optimization of internal spur gear design using genetic algorithm," International Journal of Mechanical Engineering, **2**, 22-30

10. Shigley, J. E., Mischke, C. R., Budynas, R. G. 2004, Mechanical Engineering Design, McGraw-Hill, New York, Chap. 14

11. http://mechanote.blogspot.com

12. http://www.roymech.co.uk/Useful_Tables/Drive/Gears.html

13. http://nuvvo.com/lesson/7611-a-comprehensive-lesson-on-gears

14. http://www.expertsmind.com/topic/gear-geometry/involute-profile-teeth-98696.aspx

15. http://www.automation.com/library/articles-white-papers/motion-control/engineering-reference-stealth-helical-planetary-gearhead-technology

16. http://web.itu.edu.tr/~fetvacic/femgear/modeles1.htm